12-2006

Processing and Characterization of a Novel Bioabsorbable Polymer for Biomedical Applications

Katherine Atchley
University of Tennessee - Knoxville

To the Graduate Council:

I am submitting herewith a thesis written by Katherine Atchley entitled "Processing and Characterization of a Novel Bioabsorbable Polymer for Biomedical Applications." I have examined the final electronic copy of this thesis for form and content and recommend that it be accepted in partial fulfillment of the requirements for the degree of Master of Science, with a major in Engineering Science.

Joseph E. Spruiell, Major Professor

We have read this thesis and recommend its acceptance:

Roberto S. Benson, Kevin M. Kit

Accepted for the Council:
Carolyn R. Hodges

Vice Provost and Dean of the Graduate School

(Original signatures are on file with official student records.)

To the Graduate Council:

I am submitting herewith a thesis written by Katherine Atchley entitled "Processing and Characterization of a Novel Bioabsorbable Polymer for Biomedical Applications." I have examined the final electronic copy of this thesis for form and content and recommend that it be accepted in partial fulfillment of the requirements for the degree of Master of Science, with a major in Polymer Engineering.

Joseph E. Spruiell

_____

Major Professor

We have read this thesis
and recommend its acceptance:

Roberto S. Benson

Kevin M. Kit

Accepted for the Council:

Anne Mayhew
Vice Chancellor and
Dean of Graduate Studies

(Original signatures are on file with official student records.)

Processing and Characterization of a Novel Bioabsorbable Polymer for Biomedical Applications

A Thesis

Presented for the

Master of Science Degree

The University of Tennessee, Knoxville

Katherine Marie Atchley

December 2006

Dedication

This thesis is dedicated to my parents, Keith and Susan Morris. Their love and support gave me the courage to attempt a Masters degree in a new field, and their encouragement kept me going through the difficult times. Thank you for believing.

Acknowledgements

I would like to take this time to thank everyone who helped me complete my Master of Science degree in Polymer Engineering. Most especially, I would like to thank Dr. Spruiell for his help and guidance throughout my graduate studies. I would also like to thank Dr. Kit and Dr. Benson for serving on my committee, and Dr. Harper for working so closely with me towards the end of my research. Finally, I would like to thank Mike Neil and Doug Fielden. Without their technical support none of this would have been possible.

Abstract

A series of amino acid based bioanalogous polymers have been synthesized by Dr. C. C. Chu at Cornell University for future use in biomedical applications. These poly(ester amide)s have been designed to be bioabsorbable, with particular interest in internal fixation and drug delivery applications. The polymers PEA 4-Phe-4, 4-Phe-Das, and 8-Phe-Das were studied; however, due to better material properties, the focus mainly centered on 4-Phe-4. Since these are new polymers, processing conditions needed to be determined and the structure and properties characterized. The fibers were also processed post-extrusion in an effort to induce orientation and crystallinity within the polymer chains.

All three PEAs were extruded into monofilament fibers by way of a single-screw extruder. The 4-Phe-4 was processed at temperatures ranging from 150° – 195°C, and the 4-Phe-Das and 8-Phe-Das were processed at 135° and 140° C respectively. Post-extrusion drawing and annealing resulted in an increase in orientation, however crystallinity could not be induced by these methods. A nucleating agent was mixed with the 4-Phe-4 which seemed to result in an increase in the elastic modulus of the fiber. As with the drawing and annealing, the polymer remained amorphous following the addition of the nucleating agent.

Basic material properties were obtained for all three polymers. PEA 4-Phe-4 has a T_g of 59°C and a T_m of 109°C in its as received form. Once spun, the T_m disappears and the T_g lowers to 52±1.5°C. This loss of T_m corresponds to wide angle x-ray diffraction data collected and reinforces that the fibers are indeed amorphous. The 4-Phe-4 fibers have an elastic modulus ranging from 1606±188 MPa for the as spun fiber to

1919±203 MPa for the most highly drawn fiber. Similarly, the yield strength ranges from 11.4±0.75 – 113.1±22 MPa, and ultimate tensile strength ranges from 73±5 – 215±22 MPa. Birefringence ranges from 0.0026±0.00023 – 0.01812±0.00053. Dilute solution viscosity measurements provide an intrinsic viscosity of 0.55 dL/g for the as received polymer and 0.44 dL/g for the spun fibers.

Sodium benzoate was used as a nucleating agent during melt spinning. Once the nucleating agent was mixed with the 4-Phe-4, the T_g decreased further to 48°C. As before, there was no T_m present, which was confirmed by the WAXD data. The elastic modulus increased to 4246±430 MPa for the spun fiber and 5763±458 MPa for the fibers most highly drawn. The yield strength is within the same range as the original 4-Phe-4 fiber within reasonable error, ranging from 52±13 – 101.5±5 MPa. The ultimate tensile strength decreased, however, ranging from 63.5±2 – 122±17 MPa. Birefringence values were also slightly lower than the pure 4-Phe-4, ranging from 0.00168±0.00012 – 0.01488±0.0017.

Finally, pure 4-Phe-4 was compression molded into film and drawn using a biaxial stretcher. Birefringence measurements for the drawn film are low compared to similar draw ratios in the fiber, ranging from 0.0011±0.00006 – 0.0042±0.00021. These drawn film samples were also subjected to creep testing using a DMA. Results show that 4-Phe-4 creeps at 37°C under a constant load.

The 4-Phe-Das and 8-Phe-Das behaved similarly throughout testing. Both polymers have low intrinsic viscosities (0.27 dL/g for both. The T_g for both is approximately 40°C in the as received form, and 58±0.5°C once spun into fiber. As spun 4-Phe-Das fibers have an elastic modulus of 2337±518 MPa, an ultimate tensile strength

of 100±8 MPa, and a birefringence of 0.00341±0.0023. Corresponding data for 8-Phe-Das fibers reveal an elastic modulus of 1761±407 MPa, an ultimate tensile strength of 63±6 MPa, and a birefringence of 0.00103±0.0003.

Drawing appeared to provide some short range order and orientation within both the pure and nucleated 4-Phe-4 fibers. This can be seen to some extent through WAXD, but is most noticeable in the birefringence data. This chain orientation also leads to a significant increase in mechanical properties. Due to extreme brittleness, the 4-Phe-Das and 8-Phe-Das polymers were unable to be drawn, and their mechanical and optical properties suffered. Annealing did not have as great of an effect on the mechanical properties as drawing, but shrinkage tests conducted in heated water confirm that annealing helps to stabilize the fiber length and reduces shrinkage when heated above the T_g of the polymer.

The method of processing seemed to give the 4-Phe-4 fibers an advantage over the film when measuring their optical properties. Both fiber and film were drawn to similar draw ratios, yet the birefringence values of the drawn fiber are much higher than those of the drawn film. It seems that the initial orientation provided by the melt spinning processes lead to greater orientation during drawing. It is also likely that the higher draw temperatures for the film allowed the chains more freedom during drawing, therefore lowering their overall orientation.

Creep studies conducted at physiological temperature (37°C) show that the 4-Phe-4 film creeps significantly under constant load for prolonged periods of time. This may make the idea of application in a drug delivery system more feasible than internal fixation.

Table of Contents

Table of Tables

Table of Figures

Chapter 1. Introduction

Interest in reducing wound healing time with drug delivery devices and preventing multiple surgeries due to a need to remove internal fixation implants has lead to the need for biodegradable polymers that are biocompatible both as a whole and as they degrade. Therefore, polymers composed of naturally occurring building blocks are gaining popularity for use in biomedical applications. In addition to good biocompatibility, these materials need to be affordable during synthesis, processing, and while undergoing purification and sterilization. With these goals in mind, a new series of poly(ester amide)s is being developed by Dr. C. C. Chu at Cornell University. These advanced PEAs are biologically active, and have promising biocompatibility properties. The basic tasks considered throughout the entirety of this project are: chemical synthesis of the new PEAs with characterization of their chemical, physical, and thermal properties, melt spin these PEAs into fiber, fiber characterization that evaluates the structural, physical, mechanical, thermal, biodegradability, and morphology, *in vitro* biodegradation studies, and *in vivo* biodegradation studies. [16]

The synthesis and characterization related to biodegradation, as well as the *in vitro* and *in vivo* studies, are being conducted by Dr. Chu and his colleagues at Cornell University. The focus of this paper is the development of melt spinning conditions and the characterization of the resulting fiber. A total of three PEAs were studied in this research, but the majority of the research focused on PEA 4-Phe-4. The structural, thermal, mechanical, and optical properties were cataloged following each change in processing, from the initial extrusion through changes in chain conformation due to

annealing and drawing. Preliminary creep studies were also conducted on compression molded film that had been drawn. Effort was made throughout this study to induce crystallinity and orientation in order to make a more desirable fiber. In addition to annealing and drawing the as spun fibers, methods for inducing crystallization during processing were employed. A solution spinning processing approach was attempted for inducing crystallinity through solvent effects, and a nucleating agent was mixed into the polymer during melt spinning to attempt to grow crystals from the melt.

Chapter 2. Literature Review

2.1 Biomaterials

Biomaterials are biocompatible materials that can be used in medical devices, and are intended to interact in biological systems [1]. The material's biocompatibility means they are in no way toxic or harmful to the biological host environment [2]. In addition to basic biocompatibility, implantable polymers should be free of additives, maintain chemical stability during processing and sterilization, and they should not induce thrombosis, inflammatory encapsulation, tumor formation, or cell changes in the surrounding tissue. Biodegradable polymers must be engineered so that they maintain their biocompatibility as they biodegrade. For nondegradable implantable polymers, the material should be designed so that stability is maintained within the physiological environment. [3]

2.2 Biodegradation

A change in physical properties resulting from the chemical breakdown of a material due to living organisms is the defining characteristic of biodegradation [3]. Within the body, polymers are not only subjected to continuous or cyclic stresses, but also the biological mechanism known as immune response. The internal environment is aseptic, and maintained at 37°C with a pH of 7.4. For metals, protein adsorption on the surface of a device leads to an increase in the rate of corrosion. The oxidizing agents and enzymes released by the cells to digest the foreign materials are of concern for all

materials used in medical devices [4]. The two main types of biodegradation processes are hydrolytic and oxidative.

2.2.1 Hydrolytic Degradation

Hydrolysis, or the chain scission of susceptible functional groups due to reactions with water, is a single-step process that can be catalyzed by acids, bases, salts, or enzymes. The functional groups that are most vulnerable to hydrolysis are carbonyls bonded with O, N, or S. Examples of these include esters, amides, and carbonates. Hydrolytic tendencies can be suppressed through cross-linking, high crystallinity, and thermal annealing. Within the body, ions in the extracellular fluid have been known to catalyze hydrolysis; an affect particularly noted in polyesters. Other host response catalysts are localized changes in pH due to acute inflammation or infection and hydrolytic enzymes. However, enzymes are designed to recognize and attack certain natural chain sequences. Lacking these naturally occurring recognizable sequences, many synthetic polymers are resistant to enzymatic degradation [4].

2.2.2 Oxidative Degradation

Oxidative degradation is the chain scission of functional groups that are readily oxidized. Examples of these functional groups include ethers, phenols, alcohols, aldehydes, and amines. The primary host catalysts for oxidative degradation are phagocytic cells such as neutrophils and macrophages, which are activated by cells and sent to respond to injury and foreign body sites. Both neutrophils and macrophages can metabolize oxygen to form a superoxide anion. This is show in **Figure 1**.

OXIDATIVE DEGRADATION

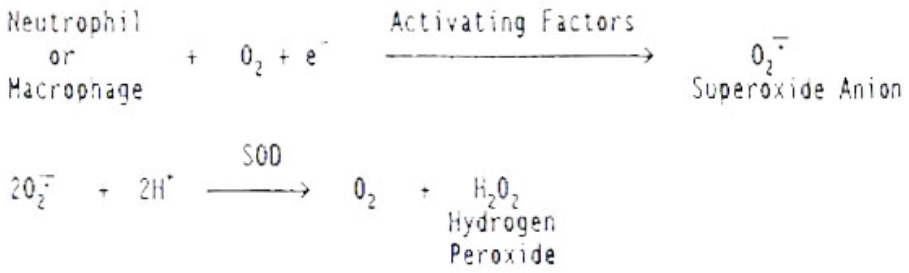

Figure 1. Oxidative Degradation - General Scheme

From here, either more powerful oxidants can be formed, or the superoxide anion can initiate homolytic reactions within the polymer. These homolytic reactions allow the material to oxidatively degrade [4].

2.3 Bioabsorbable Polymers

Bioabsorbable polymers are degradable materials that are particularly useful in short-term medical applications that only require the temporary presence of a polymer implant. In literature, the terms bioabsorbable and bioresorbable are often interchangeable. Their use implies that the degradation products of the material are processed by phagocytosis and naturally removed from the biological environment. The three most common bioabsorbable polymers are poly(glycolic acid), poly(lactic acid), and polydioxanone. These are already FDA approved for use in clinical studies involving humans, and are used routinely in medicine. Other bioabsorbable polymers include polyhydroxybutyrate, polyhydroxyvalerate, polycaprolactone, polyanhydrides, poly(ortho ester)s, poly(amino acid)s, and poly(ester amide)s [1].

2.3.1 Bioabsorbable Polymer Applications

Bioabsorbable polymers have seen great success in the capacity of a temporary scaffold. During situations where natural tissue is weakened by disease, injury, or surgery, bioabsorbable polymers can be used to provide structural support to aid wound healing, bone repair, and damaged blood vessels. Applications within temporary scaffolding include sutures, bone fixation devices, and vascular grafts. The idea behind a

temporary scaffold is that a gradual stress transfer will occur between the polymer and the healing tissue, so that as the tissue heals, the polymer slowly weakens.

A similar application is that of the temporary barrier to prevent adhesion during wound healing. Adhesion occurs between two tissues sections, and is the result of clotting blood. Inflammation and fibrosis are the end results of adhesion, which can be a major problem following surgery. If the tissue adheres incorrectly, pain and functional impairment can occur, possibly leading to further surgery to repair the bonded tissues interface. Temporary barriers take the form of a thin film or mesh. They are placed between adhesion-prone tissue at the time of surgery, and allow for more controlled wound healing. These barriers are also used with burn victims and other skin lesion conditions, where artificial skin is a necessary step towards recovery.

Drug delivery systems are implantable polymeric devices that release medicine slowly where it is most needed as the polymer degrades. This is especially common when administering chemotherapy, because the target cells can be treated without damaging cells throughout the body. There is also potential for combining the drug delivery with temporary scaffolds or barriers to create multifunctional devices that would limit surgeries and implants in patients requiring both mechanical support and site-specific drug delivery [4].

2.4 Poly(ester amide)s

Polyesters are a common class of biodegradable polymers with typically poor thermal and mechanical properties. Polyamides generally have excellent thermal and mechanical properties, but slow to biodegrade due to strong intermolecular interactions.

This inertness to biodegradation is likely due to the large concentration of hydrogen bonds and high regularity of the polyamide structure, however the amide functional groups are susceptible to enzymatic degradation. In an effort to create a biodegradable polymer with good thermal and mechanical properties, many new polyesteramide copolymers have been synthesized in recent years. [5]

Recent interest has been concerned with creating polyesteramides (PEAs) that are composed of natural building blocks so that once the polymer degrades, the degradation products can be safely metabolized by the body. Examples of these natural building blocks are α-amino acids and α-hydroxy acids. Polyamides based on α-amino acids are viewed as a promising candidate for this type of polymer due to their similarities to natural proteins. However there are several problems when working only with poly(α-amino acid)s, including expensive manufacturing processes, insolubility in common organic solvents, thermal degradation during the melt process, and slow rates of biodegradation. Poly(α-ester α-amide)s combine useful properties of poly(α-hydroxy acid)s and poly(α-amino acid)s, however the synthesis of this copolymer is expensive and complex. In addition to low yield and low molecular weight, undesirable side reactions typically occur due to the severe reaction conditions needed in the ring-opening melt polymerization. These side reactions lead to byproducts that would need to be eliminated to ensure purity of the material before it could be used in medical applications. [6]

In this study, PEAs were synthesized in the form of an AA-BB type amino acid based bioanalogous polymer. They are produced by solution polycondensation under mild conditions. Due to the building blocks used, toxic catalysts are not necessary for polymerization. The main benefit to this type of synthesis is reduced cost in producing

polymers with a wide range of material properties. Several different polymers were created by varying three main components: α-amino acid, diol, and dicarboxylic acid. A wide range of properties could conceivably be easily achieved through different combinations of these basic building blocks. Applications could range from surgical implants like vascular grafts, nerve guidance tubes, absorbable bone plates, pins and screws, surgical meshes, and temporary artificial skin to drug delivery devices. These polymers are susceptible to enzymatic biodegradation from specific enzymes (i.e. α-chymotrypsin). Typically, the rate of biodegradation is controlled by varying functional groups. For this polymer, the rate of biodegradation is controlled by the polymethylene chain length of the diol.[6]

The synthesis is achieved in a three step process: (1) preparation of di-*p*-toluenesulfonic acid salts of bis (α-amino acid) α,ω-alkylene diesters, (2) preparation of di-*p*-nitrophenyl ester of dicarboxylic acids, and (3) solution polycondensation of the products from steps 1 and 2. Six α-amino acids were used (L-Valine, L-Leucine, L-Isoleucine, DL-Norleucine, L- and DL-Phenylalanine, and DL-Methionine) with three diols (1,3-propanediol, 1,4-butanediol, and 1,6-hexanediol) and two dicarboxylic acyl chlorides (adipoyl and sebacoyl). Other components include *p*-toluenesulfonic acid monohydrate, *p*-nitrophenol, *N,N*-dimethylacetamide, *N*-methyl-2-pyrrolidinon, benzene, nitrobenzene, ethylacetate, acetone, acetonitrile, chloroform, triethylamine, *N*-methylmorpholine, *N,N,N,'N,'*-tetramethylethylenediamine, and pyridine. The polymers were named by counting the Carbons in the dicarboxylic acid (x) and diol (y), and by the α-amino acid (αaa) used (i.e. x-αaa-y). [6]

A typical characteristic of all of the PEAs synthesized by this technique are given by FTIR data. There are carbonyl bands at 1648-1650 cm^{-1} that represent amide I, 1538-1542 that represent amide II, and 1738-1742 that represent the ester group. There are also NH vibrations at 3290 cm^{-1}. For the PEA composed of phenylalanine, there are also bands at 700 and 750 cm^{-1} indicating the presence of the phenyl group. There are also two characteristic >C==O signals from C-NMR spectra that are representative for all of the adipoyl PEAs, indicating no interchange reaction between the amide and ester groups and favoring a regular structure. Were interchange reactions present, there would be more than two >C==O signals, because other types of ester and amide groups would form. This favors a regular structure, because the presence of other ester and amide groups in the backbone would lead to an irregular structure. Finally, the glass transition temperatures of all of the PEAs synthesized ranged from 11 to 59°C. Most of the polymers were amorphous, however the polymers created from phenylalanine and some from valine exhibited semicrystalline characteristics with a melting temperature in the low 100s°C. Low fusion temperatures from 20-130°C indicate that these PEAs could have an aptitude for drug delivery devices. [6]

Enzymatic degradation studies have been conducted primarily with α-chymotrypsin catalyzed hydrolysis. The enzyme α-chymotrypsin was chosen, because it would cleave ester linkages at the C-terminal of hydrophobic α-amino acids. Lipase was also used to cleave the ester bonds of the hydrophobic substrate. [7] The high hydrophobicity from the benzyl side groups in the PEAs based on L-phenylalanine lead to the highest tendency towards α-chymotrypsin catalyzed hydrolysis. Lengthening the methylene groups in the diol also lead to an increase in hydrophobicity, which in turn

lead to an increase in hydrolysis. Another increase in enzymatic sensitivity occurred due to increasing both the x of the diols and the y of the dicarboxylic acids. This leads to the conclusion that the higher the hydrophobicity of the polymer backbone, the higher the chance that the polymer will hydrolyze due to enzymatic degradation. [6]

The main PEA characterized in the present study is PEA 4-Phe-4. It is composed of adipic acid (C=4), L-phenylalanine (Phe), and 1,4-butanediol (C=4). A schematic of the structure of 4-Phe-4 is included in **Figure 2**. [8] Preliminary thermal data suggests a T_g of 59°C and a melting point in the low 100s°C. [6] The 4-Phe-4 showed a higher susceptibility to lipase than α-chymotrypsin in degradation studies. The 4-Phe-4 films were subject to surface erosion during biodegradation, but the films eroded evenly and retained their shape as they became uniformly thinner over time. Biodegradation products were tested for toxicity by creating a matrix for a bacteriophage containing artificial skin. The results suggest no acute or chronic toxicity. Based on these tests, PEA 4-Phe-4 was approved for clinical trials in the Republic of Georgia. [7] Biocompatibility of 4-Phe-4 fibers was tested in rats and compared to the commercial sutures, Monocryl (from Ethicon).

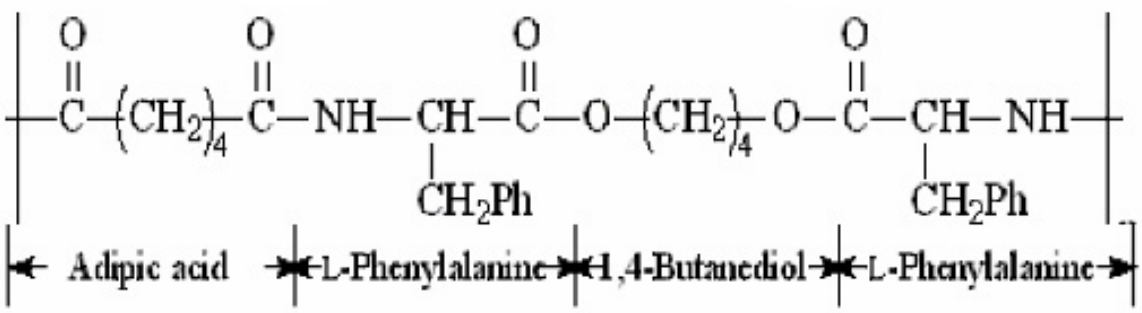

Figure 2. PEA 4-Phe-4 Structure

Fibers were implanted in the rat's gluteal muscular area and studied of a period of several days (7, 14, 28, and 42 day periods). The PEA fibers showed a significant reduction in tissue inflammation within all time periods in comparison to the Monocryl sutures. [8]

2.5 Fiber Spinning

Fibers are produced through either a melt or solution spun process that involves moving either the molten polymer or solution through a barrel and pushing it through a die. The objective is to produce long, thin, filaments of relatively constant cross-sectional area. Once spun, fibers are usually strengthened by a drawing process that takes place at a relative high stress and low temperature for the specific polymer. If a material melts without significant decomposition, the melt spinning process is used to produce fibers of an approximately constant cross-section [9]. If the polymer cannot be processed in a molten state, either a wet or dry solution spinning technique is used.

2.4.1 Melt Spinning

Melt spinning is a process that involves melting a material and extruding it through a die. The polymer cools as it exits the die and solidifies into filaments that can be wound onto a bobbin. A tensile force is typically applied to the polymer as it exits the extruder to draw the filaments down to a desired diameter [10]. The essential components of melt spinning are the screw and the die. The screw serves as a pump, pushing the molten polymer through the barrel of the extruder. It controls the rate of extrusion, and aids in mixing the still solid polymer entering the extruder with the molten

polymer flowing within. The die provides the final shape of the extrudate, and depending on the fiber application can be single or multifilament. [11]

2.4.2 Solution Spinning

For polymers that cannot form thermally stable, viscous melts, solution spinning is an alternative method of processing, provided that the polymer can be dissolved in high enough concentration in proper solvents. The polymer content of these solutions should be between 5 and 30% [12]. During solution wet spinning, a non-volatile solvent is used, and the solution is extruded into a bath containing non-solvents. As the polymer passes through the bath, it leaves the solution and becomes a solid filament before being taken up on a roll. Dry spinning utilizes a volatile solvent, which is evaporated into a gaseous environment during draw down [9].

2.4.3 Fiber Orientation

Orientation of the polymer chains is achieved when a fiber sample is heated above its T_g and drawn to a longer length. Polymer molecules can be oriented while in the nearly molten state by applying a uniaxial tensile stress or unidirectional shear stress. When properly accomplished, the resulting polymer is stiff and strong in the draw direction, but is usually quite weak in the transverse direction. If the polymer is able to crystallize, the orientation process encourages rapid crystallization due to the molecular alignment of the chains. In these cases, the crystalline structure is linear instead of spherulitic [11].

To determine the degree of orientation, birefringence measurements are taken of the fiber samples. Birefringence (Δn) is the difference in the refractive index of a material in two orthogonal directions, and is measured with linearly polarized light. The index of refraction (n) is defined by the ratio of the velocity of light traveling in vacuum to the velocity of light traveling through the material. As light reaches the interior of transparent materials, it decreases in velocity and bends at the interface [13]. The degree of bending is dependent upon the wavelength of the light, and the orientation of the material. The refractive index differs in the directions parallel and normal the chain axis due to differences in bonding. [14] If a polymer is a birefringent material, it will have a non-zero difference between the two refractive indices, and it will have a net orientation to yield a primary refractive index. Due to their large degree of ordering and anisotropy, crystalline materials are highly birefringent. Birefringence measurements can assess whether or not a material is crystalline or semi-crystalline, and if so monitor the crystal growth in studies of kinetics. [15] For preferentially oriented materials, such a fibers that have been drawn, the birefringence equals $\Delta n = n_1 - n_2 = f\Delta n^{\circ}$, where f is the Hermann's orientation function, and Δn° is the intrinsic birefringence. This orientation function is a quantitative measure of the degree of chain orientation. [14]

Chapter 3: Materials and Experimental Methods

3.1 Materials

Three poly(ester amide)s (PEAs) were provided by Dr. C. C. Chu (Cornell University, New York). In total, approximately 450 grams of PEA 4-Phe-4, 630 grams PEA 4-L-Phe-Das, and 650 grams PEA 8-L-Phe-Das were processed and characterized. Throughout this paper, these polymers will be referred to as 4-Phe-4, 4-Phe-Das, and 8-Phe-Das. The structure for 4-Phe-4 is shown in Figure 1, but the exact composition has never been provided. The structures for 4-Phe-DAS and 8-Phe-DAS were never provided, however based on the naming convention both are composed of phenylalanine. The 4-Phe-DAS is made of adipic acid, while the 8-Phe-DAS is made of sebacic acid. The diol building block used for these polymers is unknown. The solvents n,n-dimethyl formamide (A.C.S. grade) and chloroform (HPLC grade) were used to create PEA solutions, and ethyl acetate (Reagent A.C.S. grade) was used in the coagulation bath. The nucleating agent sodium benzoate (laboratory grade powder) was also used.

The naming convention used throughout this paper is built upon the basic polymer names given above. For the spun fiber, an F is added onto the end of the name. Depending on further processing, a draw ratio or annealing temperature is then listed. A nucleating agent was incorporated into some of the fibers. To differentiate between these fibers and the original as spun fiber, an N is used instead of an F. For the film, CM is used in place of F, which stands for compression molded. Also, a U or C is placed before the draw ratio for the film samples to differentiate between constrained and unconstrained drawing conditions. An example of each of these is shown in **Table 1**.

Table 1. Naming Convention

Name	Description
4-Phe-4	As Received Polymer
4-Phe-4-F	As Spun Fiber
4-Phe-4-N	Nucleated As Spun Fiber
4-Phe-4-F-2x	2x Drawn Fiber
4-Phe-4-N-2x	2x Drawn Nucleated Fiber
4-Phe-4-F-A68	Fiber Annealed at 68°C
4-Phe-4-F-4x-A68	4x Drawn Fiber Annealed at 68°C
4-Phe-4-CM	Compression Molded Film
4-Phe-4-CM-U4x	4x Drawn (Unconstrained) Film
4-Phe-4-CM-C4x	4x Drawn (Constrained) Film

3.2 Processing

3.2.1 Melt Spinning

The as received polymer was dried under vacuum for at least 8 hours at 50°C prior to extrusion. Melt spinning was conducted using a single screw Brabender extruder with a single filament die. The extruder was not equipped with a constant displacement gear pump, or a nitrogen purge. There were three heating zones maintained during extrusion: the barrel near the hopper, the central portion of the barrel, and the die. The temperature settings for these zones are listed in **Table 2** for each spinning process. Once polymer had been pushed through the barrel by the screw, a sample of the extrudate was taken over a period of time to determine the mass throughput. Due to the lack of gear pump, mass throughput could not be kept constant, so this measurement was an approximation. The Brabender extruder is shown in **Figure 3**.

3.2.2 Solution Spinning

The solution spinning setup consisted of a motorized press that was used to push the plunger of a syringe at a constant rate. The extrudate from the syringe was pushed into a coagulation bath of ethyl acetate. A take-up roll was attached to the end of the bath. Solutions were made using 3 grams of as received polymer and 20 mL of solvent. Both chloroform and n,n-dimethyl formamide were used to create solutions.

3.2.3 Compression Molding

Thin film was formed using a Wabash (Wabash, IN) Hydraulic Press. The platen heaters were set to 140°C (284°F) for the as received 4-Phe-4.

Table 2. Melt Spinning Parameters

Polymer	Bobbin	Temperatures (°C)			Take Up Speed (rpm)
		Hopper	Barrel	Die	
4-Phe-4-F	1	120	180	195	296
	2	120	175	187	270
	3	120	172	181	240
4-Phe-4-N	1	110	140	150	196
	2	110	140	150	346
	3	110	140	150	240
4-Phe-Das	1	100	130	135	455
	2	100	130	135	560
8-Phe-Das	1	103	133	140	392
	2	103	133	140	By Hand

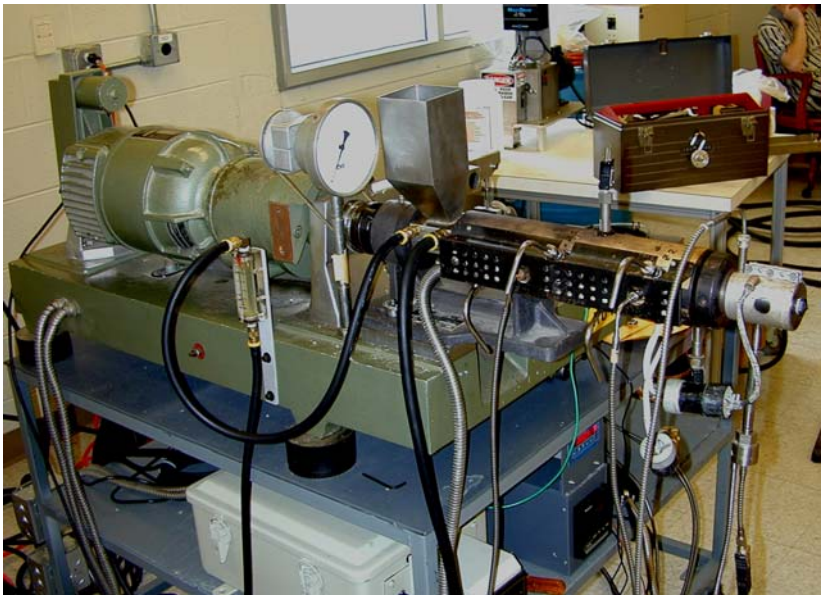

Figure 3. Brabender Extruder

To press the film, approximately 4 grams of polymer were placed between two sheets of Kapton (DuPont) polyimide film, and placed on the press. The platens were brought together so that the upper platen just touched the upper sheet of Kapton. The platens were held in this position for five minutes to give the polymer time to melt. At the end of the melt time, the platens were brought together at a pressure of approximately 1.5 tons for another five minutes. Once fully pressed the platens were separated, and the polymer film was quenched in a room temperature water bath. The as received polymer was dried under vacuum for 8 hours at an oven temperature of 70°C prior to compression molding.

3.2.4 Post-extrusion Drawing

Fiber samples were drawn through three sets of rotating, heated rolls. The drawing apparatus is setup to take fiber directly from the bobbin, pull it across the series of rolls, and rewind it on a take-up roll post drawing. For the 4-Phe-4-F, samples from bobbin 1 were initially drawn by hand across rolls 1 (56°C, 15 rpm) and 2 (52°C, 30 rpm). This was repeated to produce an approximate 4x draw ratio, and a more highly drawn fiber of approximately 6x. Another round of hand drawing occurred with fiber from bobbin 3. These drawn fibers are the filaments predominately used through the characterization tests. Conditions for the second round of drawing were: roll 1 (48°C, 24 rpm) and roll 2 (47°C, 40 rpm). The 4-Phe-4-N wound much easier off the bobbin, and was pulled through all three sets of rolls. The drawing conditions are included in **Table 3**, while the drawing apparatus is shown in **Figure 4**.

Table 3. Nucleated 4-Phe-4 Drawing Conditions

Drawing Conditions				
Polymer	Bobbin	Roll 1	Roll 2	Roll 3
		50 C	48 C	40 C
4-Phe-4-N	2x	15	28	28
	3x	15	44	42
	2.5x	14	36	36

Figure 4. Drawing Apparatus

3.2.5 Post-extrusion Annealing

Fibers were annealed in a Fisher Scientific Isotemp Vacuum Oven Model 285A. They were annealed under vacuum for 1.5 hours at three different temperatures. Glass sample holders were used to maintain constant length, as well as to ensure there could be no burning from the fiber coming into contact with metal. The temperatures used were: 77°, 72°, and 68°C for the 4-Phe-4, and 65°C and 70°C for the 4- and 8-Phe-Das. These temperatures were chosen based on the DSC thermograms. They are high enough above T_g to illicit rubbery response, yet they are lower than the onset of the melting peak in the as received 4-Phe-4.

3.2.6 Post-molding Stretching

Compression molded film samples were cut into 59 mm squares. To stretch the film, the T. M. Long biaxial stretcher heaters were set to a temperature of 110°C. After loading the film, the samples were allowed a 2 minute wait to acclimate to the heat of the chamber before being stretched. The samples were uniaxially stretched at a constant rate in both constrained and unconstrained conditions. Biaxial stretching was not attempted.

3.3 Characterization Techniques

3.3.1 Wide Angle X-Ray Diffraction

Wide angle diffraction patterns were collected using the Molecular Metrology SAXS/WAXS system. This was accomplished by exposing the as received and fiber samples to radiation for 1 hour and collecting the scatter with an image plate. The SAXS/WAXS system utilizes a CuKα (1.5419 Å) x-ray source through a typical three-

pin-hole system. The first pinhole has a diameter of 0.4 mm, the second is 0.2 mm, and the guard pinhole is 0.7 mm in diameter. The system operates under vacuum at 45 kV and 0.66 mA, and uses a double focusing mirror to enhance intensity. The sample to film distance is approximately 36 mm, and the image plate was scanned with a Fuji BAS-1800II image analyzer. The resulting pattern was converted to an intensity versus 2θ plot by Polar x-ray analysis software.

3.3.2 Thermal Analysis (TGA and DSC)

A Perkin Elmer Pyris 1 TGA Thermogravimetric Analyzer was used to provide a basic understanding of the thermal degradation of the 4-Phe-4 in nitrogen atmosphere. Testing was conducted from 25° to 500°C with a heating rate of 20°C/minute. An aluminum pan was used to hold the sample which had an initial weight of 3.434 mg.

To determine T_g and T_m, a Mettler Toledo Differential Scanning Calorimeter 821^e with a nitrogen gas purge was used. Aluminum pans were filled with 3.75 – 5.00 mg of polymer sample. The lids of these pans were then crimped on, and three holes were poked in the top to allow for the nitrogen purge. The system was set to run from 25° to 160°C with a heating rate of 10°C/minute. One trial of as received polymer was measured as it was heated to 160°, cooled back to 25°, and then reheated to 160°. This was an attempt to discover the temperature at which the polymer crystallizes. For this trial, a cooling rate of 10°C/minute was used. The DSC instrument was calibrated using an indium standard (ΔH=28.45 j/g; T_m=156.61°C).

3.3.3 Optical Characterization (Birefringence)

The optical birefringence of the fiber samples was measured using an Olympus BH-2 Polarizing microscope with a Berek compensator. The birefringence measurements for the film were collected using the apparatus shown in **Figure 5**. The procedure for both setups was the same. A polarized film was placed between the light source and the sample holder. The sample was rotated so that the points of lowest light emission could be found. Once these "darkest points" were established, the sample was rotated 45° in both the clockwise and counterclockwise directions to measure the retardance. A compensator was used to measure the retardance of the fiber or film, and these values were manipulated to compute the birefringence values.

3.3.4 Mechanical Characterization (Tensile Testing)

The samples were loaded into a United Calibration Corp (Huntington Beach, CA) tensile tester (Model: SSTM-1-E-PC) using a 10 lb load cell and a crosshead speed of 1 in/min. Six samples were measured for each fiber sample set.

3.3.5 Dynamic Mechanical Analysis (DMA)

Creep tests were conducted using a Perkin Elmer Diamond DMA. A constant, static load of 50% of the maximum yield stress measured at room temperature was used for the creep tests. This load was 2.86 N. The Diamond DMA is set to run under constant strain, so in order to maintain the constant 2.86 N load, an initial force amplitude was set to 1000 mN, and an amplitude of oscillation during testing was set to 5.0 μm.

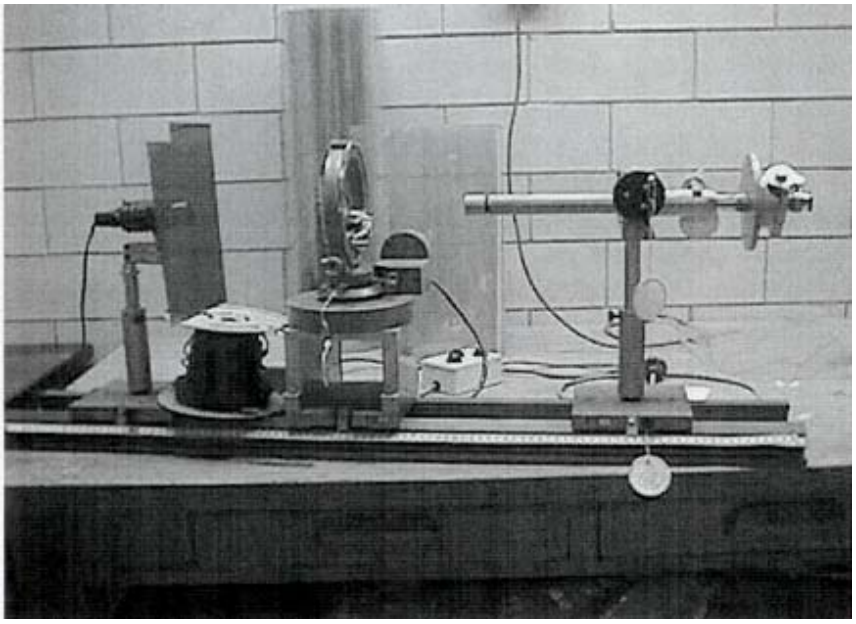

Figure 5. Film Birefringence Apparatus

Testing was carried out at 37°C to mimic application temperature within the body. Total time for each test was 180 minutes.

3.3.6 Dilute Solution Viscometry

Degradation was tested by measuring intrinsic viscosity using a Cannon CT-1000 Constant Temperature Bath and Ubbelohde viscometer. The PEA was dissolved in the solvent dimethyl formamide (DMF) for all viscosity tests. The solutions were composed of 1 g of PEA to 150 mL of DMF. Once a sample solution was fully mixed, 10 mL was pipetted into the No 1: 420 Ubbelohde viscometer. Efflux times were measured according to ASTM standard D2857. The efflux time of DMF was measured before each sample trial set. Each trial set included five dilutions of the original 1g PEA/150 mL DMF solution. All efflux times were measured with the viscometer suspended in a constant temperature bath set to 30°C.

3.3.7 Melt Flow Indexing

To determine melt flow rate, the Dynisco: Kayeness Polymer Test Systems Series 4000 Melt Flow Indexer was used. The melt flow indexer was used several times with barrel temperatures ranging from 120° – 230°C for each trial. The load was constant at 2.16 kg. The die was plugged while the polymer melted to ensure that there was no loss before the trial began. Each melt flow rate measured was taken with a cut time of 60 seconds. Approximately 4 grams of polymer was used for each trial.

3.3.8 Hydrolysis and other Reactions to Water

Hydrolysis studies were conducted on 4-Phe-4 2x spun fibers. Water temperatures were set to 40°C in a 1L beaker. Strands of fiber were tied to a 2 ½ inch sample holder and submerged for varying periods of time. Exposure times were 1 hour, 1 day, 5 days, and 10 days. Once removed, the samples were placed on slides and optical birefringence measurements were used to determine changes in orientation due to water interactions.

Shrinkage tests were conducted on 4-Phe-4 as spun and drawn fibers. This process was accomplished by filling a 1L beaker with water and heating it to 75°C. A small metal ring weighing 0.223 g was tied to the end of a single strand of the 6x drawn fiber from spun bobbin 1. Two marks were drawn on the strand in red ink 2 inches apart. The metal ring was dipped into the 75° water until the two red marks were submerged, and immediately pulled back out. This was done to straighten the strand. Then, holding the metal ring, the strand was submerged past the 2 marks for approximately 10 seconds and removed. The distance between the two marks was measured, and the experiment was repeated with strands of undrawn fiber.

Chapter 4: Results and Discussion

4.1 PEA 4-Phe-4

4.1.1 Melt Flow Indexing

Melt flow indexing was conducted to determine the melt processing conditions and to determine the affect of prolonged exposure to heat on the polymer. Preliminary DSC tests revealed a melting peak around 110°C. An initial temperature of 125°C was chosen for the melt flow barrel, because it was about 15° above the T_m and was thought to be a good starting point for determining melt spinning parameters. Unfortunately, the polymer would not pass through the die at this low temperature. Temperature was increased slowly until the polymer started to extrude, and the final temperature was near 200°C.

Several sets of 4-Phe-4 melt flow data were collected under different conditions. Three of these trials were of great interest. The first used reheated extrudate to determine degradation. Each reheated sample was subjected to the same melt (90 seconds) and cut times (60 seconds), however three different temperatures (190°, 200°, and 210°C) were used. This trial was significant in that the amount of degradation upon reheating could be quantified from the viscosity data. The second major trial was a temperature trial. This was used to determine the best processing temperature for melt spinning. The third trial was a time trial. The best temperature from the second trial was used at various melt times. These melt times ranged from 90 seconds to 24 minutes, the latter being more realistic for extruding conditions. The results from the temperature and time trials are shown in **Figures 6** and **7**.

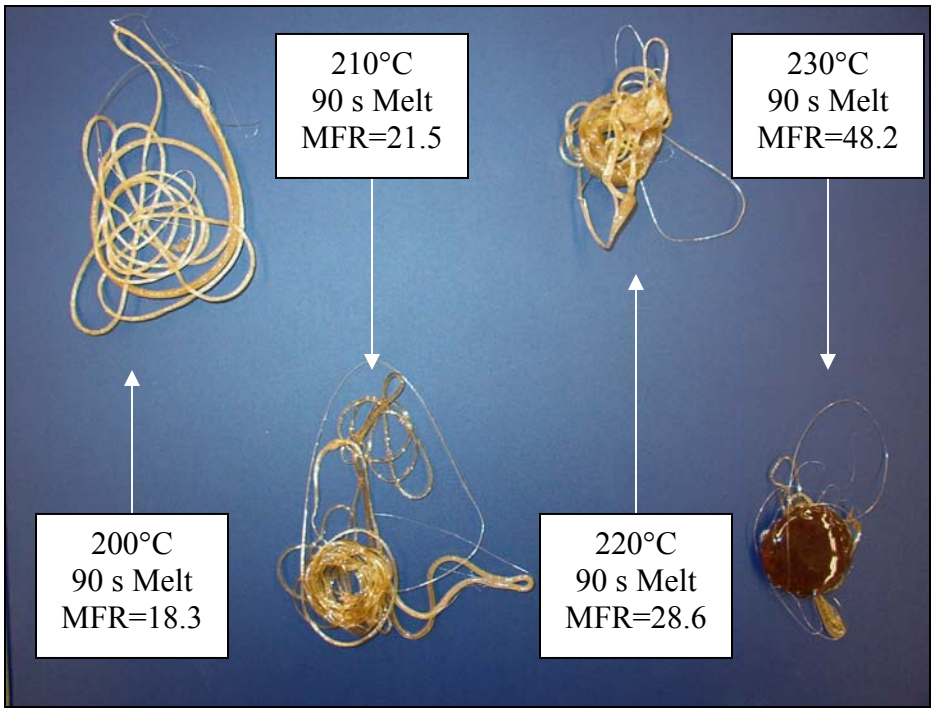

Figure 6. Melt Flow 1

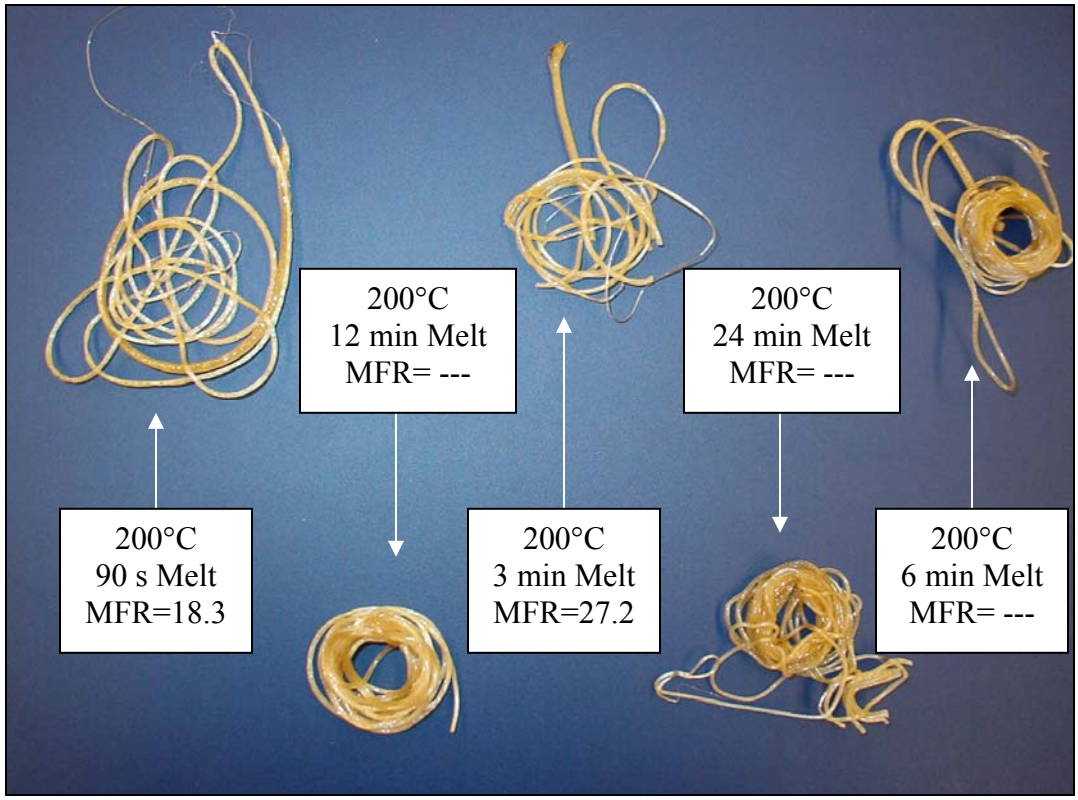

Figure 7. Melt Flow 2

For some of the higher temperatures and times, the melt flow rate was unreliable due to the fact that all of the polymer had been expelled from the barrel before the 60 second cut time was up. For these samples, the melt flow rate has been left blank. All melt flow rates are in units of g/10 minutes.

From the two figures shown, it is clear that as melting temperature and time increase, the quality of the extrudate decreases. In all of the extrudates, small bubbles were dispersed throughout the sample upon expulsion from the die. This is seen most clearly in **Figure 6** with the 200°C, 90s melt time sample. The increasing of the temperature and melt time for the trial results shown in **Figures 6** and **7** was done to try and eliminate these bubbles and defects, as well as to learn at what temperature the polymer started to degrade.

4.1.2 Thermogravimetric Analysis

TGA was performed as a preliminary test, and was only conducted in an effort to verify the degradation temperatures found from Melt Flow Indexing. The polymer appears to undergo a very little weight loss throughout the range of temperatures used in the melt flow indexing study. The onset of degradation occurs at approximately 370°C, as shown in **Figure 8**. When compared with the MFI data presented in section 4.1.1, this shows that while the quality of the extrudates decreased as the temperature was raised above 200°C, true degradation had not become serious. These high temperatures far exceed those used during melt spinning, and provide evidence that little to no degradation occurs during the spinning process.

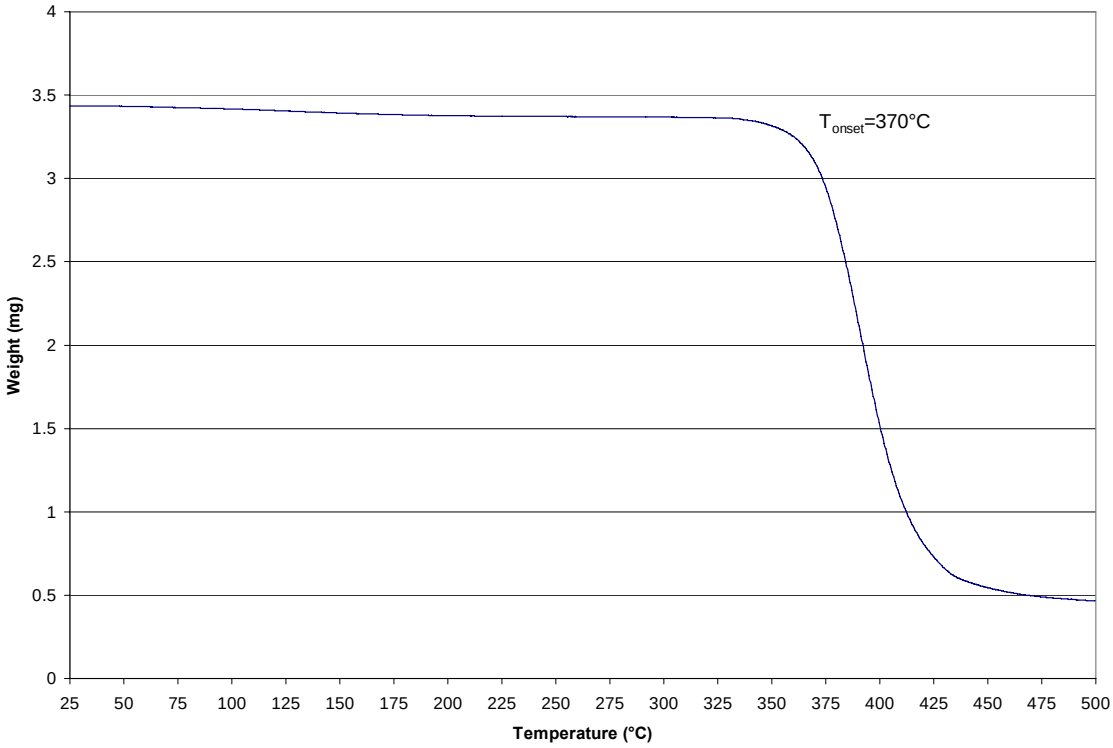

Figure 8. 4-Phe-4 TGA Scan

4.1.3 Dilute Solution Viscosity

For each sample, 10 efflux times were measured and averaged together. The reduced and inherent viscosities were calculated and plotted, and the intrinsic viscosity was taken from the y-intercept of these two charts.

Reduced Viscosity was calculated by the following equation:

$\eta_{red}=\eta_{sp}/c$ c=concentration; $\eta_{sp}=(t-t_0)/t_0$ → specific viscosity.

Inherent viscosity was calculated by the following equation:

$\eta_{inh}=(\ln \eta_r)/c$ c=concentration; $\eta_r=t/t_0$ → relative viscosity.

A representative chart with the reduced and inherent viscosity lines is shown in **Figure 9**. None of the charts looked quite like the viscosity charts shown in ASTM D2857 due to the fact that both of the lines have a positive slope. A representative chart from literature shows η_{inh} with a negative slope while η_{red} has a positive slope.

The intrinsic viscosity data for all sample groups is shown in **Table 4**. These values were calculated by taking the average of the y-intercept values from both the inherent and reduced viscosity lines.

The intrinsic viscosity value given by Dr. Chu for the as received 4-Phe-4 polymer was 0.7 dl/g, however the testing conditions were not provided. All efflux times were measured in this study were taken in a constant temperature bath set to 30°C, therefore, no data was collected to discuss variation in viscosity due to temperature.

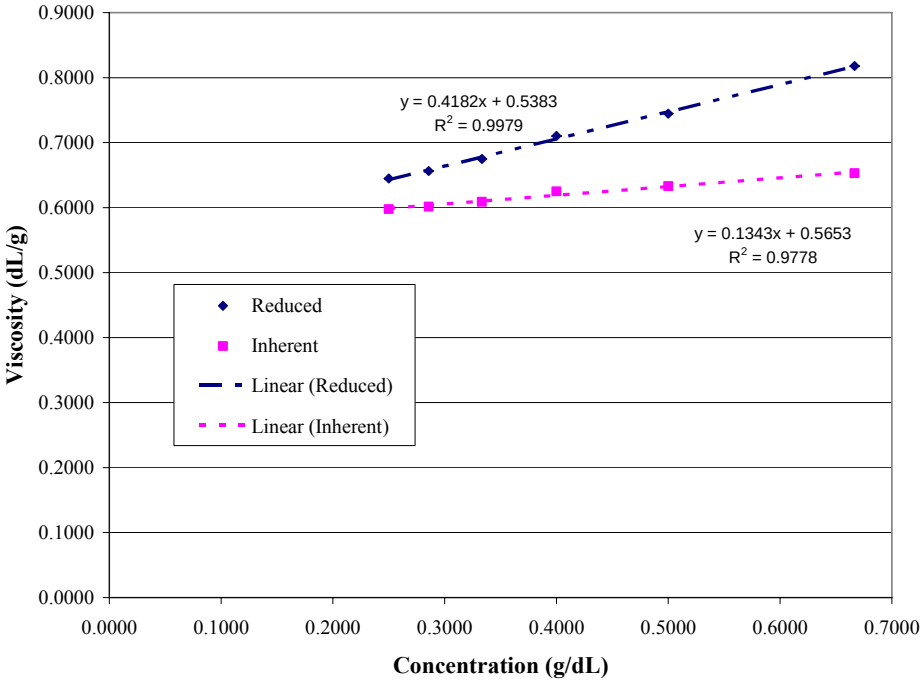

Figure 9. As Received 4-Phe-4 Viscosity Data

Table 4. Intrinsic Viscosity Values at 30°C

Sample	[η] dL/g
As Received 4-Phe-4	0.55
Spun 4-Phe-4	0.44
Nucleated 4-Phe-4	0.51
As Received 4-Phe-Das	0.27
Spun 4-Phe-Das	0.27
As Received 8-Phe-Das	0.27
Spun 8-Phe-Das	0.26
4-Phe-4 (24 min Melt Time)	0.47
4-Phe-4 Reheated (190 C in MFI)	0.53
4-Phe-4 Reheated (200 C in MFI)	0.47
4-Phe-4 Reheated (210 C in MFI)	0.46

However, it would stand to reason that there would be a significant change in the intrinsic viscosity value as temperature is increased or decreased. Variations in temperature could account for the differences between the intrinsic viscosity values measured and the values provided.

The data in **Table 4** shows that while many things were done to the polymer, the viscosity values did not change by much. Therefore, it can be reasonably concluded that degradation during processing was minimal, and these results are consistent with the TGA data presented in **Figure 8**. This is significant due to the fact that since supplies of the PEAs are limited, already spun fibers can be melted down and reprocessed if needed without much loss to the structural integrity of the polymer.

4.1.4 Melt Spinning

Based on the temperatures determined through the melt flow indexing experiments, PEA 4-Phe-4 was melt spun into a fairly brittle fiber. Unlike the three species of PEA tested in the summer of 2003 by Hua Song, the PEA 4-Phe-4 was not sticky, therefore, it did not need the application of stearic acid before winding on the bobbin. The lack of a regulator in the extruder meant poor regularity in fiber diameter throughout each bobbin. Three bobbins were spun with an approximate fiber diameter of 0.127±0.08 mm.

The nucleating agent, sodium benzoate, was incorporated into some of the as received 4-Phe-4 in an effort to induce crystallinity. There has been great success with using nucleating agents in polypropylene to regulate the size of the crystallites as well as the rate of crystallization.[20] With polypropylene, many organic and inorganic

compounds can act as a nucleating agent during processing into fibers. [19] In an attempt to mimic this process in PEA 4-Phe-4, 3.38 grams of nucleating agent was mixed thoroughly with 225 grams of as received 4-Phe-4 that had been run through a mill to decrease its particle size. The addition of the sodium benzoate and changes in spinning conditions allowed for an easier spinning process, because the filament was less prone to breaking. However, the fiber looked hazy from particles where perhaps the polymer had not fully mixed with the nucleating agent. It is likely that increases in fiber quality and strength were due to improvements in the spinning conditions. Temperatures were lowered approximately 40° in the die, which likely contributed to the increased spinnability and decreased brittleness.

4.1.5 Solution Spinning

The solution spinning setup initially involved dissolving the 4-Phe-4 in chloroform and using ethyl acetate as the coagulation bath. However, the 4-Phe-4 would not dissolve completely into the chloroform, and instead of a solution, a gel was formed. Attempts were made to push the gel through a syringe into the coagulation bath, but the gel was too inconsistent. The gel contained small pockets of air that disrupted the extrusion process. The polymer did coagulate in the bath, but it was discontinuous and could not be made to form fiber. Next, DMF was used in place of chloroform to produce a better solution. The 4-Phe-4 dissolved fully into the DMF, and coagulated fairly well into a bath of water. There were problems in removing excess air from the syringe and pushing the plunger fast enough to keep up with the flow once the solution left the needle. The DMF achieved results similar to the chloroform, in that discontinuous

polymer coagulated, but no fiber was formed. All solutions tested so far were composed of 3 grams of polymer per 20 mL of solvent. Changing the percentage of polymer in solution, determining the best coagulation bath for DMF, and perfecting the syringe method are all steps that could improve the results of this experiment.

4.1.6 Drawing and Annealing

For the 4-Phe-4, there are 3 drawn sample sets total. From bobbin 2, a 2x sample was drawn along the machine and wound on the attached bobbin. Bobbin 2 had a slightly smaller diameter due to faster take-up speeds, and produced fibers that more easily unwound from the bobbin. All other pure 4-Phe-4 fibers were hand drawn across the rolls due to breakage issues with the fiber coming off the bobbin. A set of 4x and 6x samples from bobbin 1 were hand drawn, but not closely measured for diameter, therefore these draw ratios are only an estimation. These samples were subjected to DSC, x-ray, and shrinkage analysis. One sample of the highly drawn 6x fiber was annealed at 68° and shrunk. A final set of samples was hand drawn from bobbin 3. These samples were closely characterized, so accurate draw ratios are listed throughout this paper. These samples were used for mechanical and optical testing.

Four sample sets of 4-Phe-4 were annealed. Among these, 3 have been subjected to DSC and x-ray analysis, and the other has been shrunk. The results for these tests are included in the sub-sections below.

The nucleated 4-Phe-4 fibers drew fairly easily compared to the fibers above. Breakage was still an issue, but for the most part, it occurred farther down the draw line and not at the bobbin. Fiber was successfully drawn at 2x, 2.5x, and 3x draw ratios.

4.1.7 Differential Scanning Calorimetry

DSC scans were taken of the 4-Phe-4 as received polymer, spun fiber, and modified fiber. Of these, only the as received polymer on the initial heating displayed a melting temperature. Each chart has a glass transition temperature, however on the fibrous samples it appears as a peak in the curve instead of a rise. The T_g value for the dry as received polymer is 59.2±0.14°C, the T_m value is 109.44°C, and the heat of fusion is 117.81 mJ. This is consistent with the values reported by Chu et al. [6] **Figure 10** contains the as received polymer scan from 25° to 160°C.

The data from the as received sample that was heated to 160°, cooled back to 25° and then reheated to 160°C is shown in **Figure 11**. The purpose of this scan was to determine the crystallization temperature range of the polymer. As can be seen in the thermogram, crystallization does not occur during cooling, or upon reheating. Some polyesteramides show a marked affinity for chloroform, leading to a tendency to form regular conformations within the solvent.[7] Chloroform was used during the synthesis of the PEAs studied here, so this melting peak in the as received polymer may be the result of a solvent effect. Once the polymer has been melted, this is no longer a factor.

The fibrous samples did not show a melting point, however each displayed a glass transition temperature. This temperature was fairly consistent throughout all of the charts, and the T_g value for the fibrous samples is 51.9±1.5°C. This is an average of the values collected from the three drawn samples and the three annealed samples. **Figure 12** contains a chart of the three drawn samples plotted together for comparison. **Figure 13** shows the same with the annealed samples. The T_g was expected to increase following the processing of the polymer into fiber.

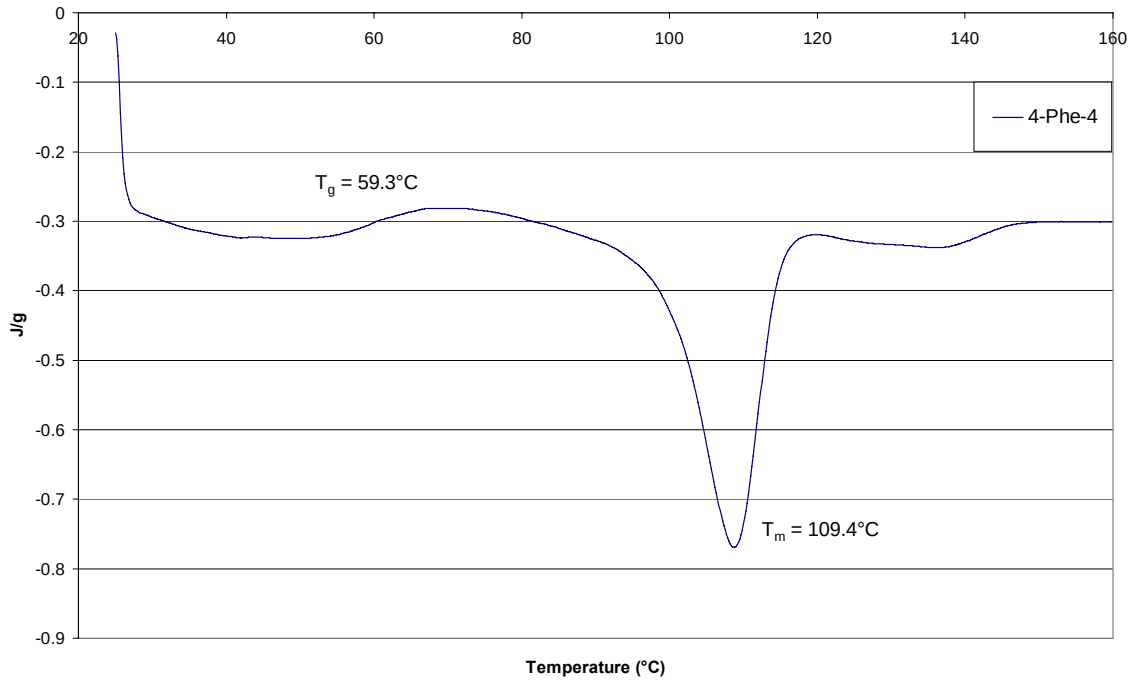

Figure 10. DSC As received 4-Phe-4 Scan

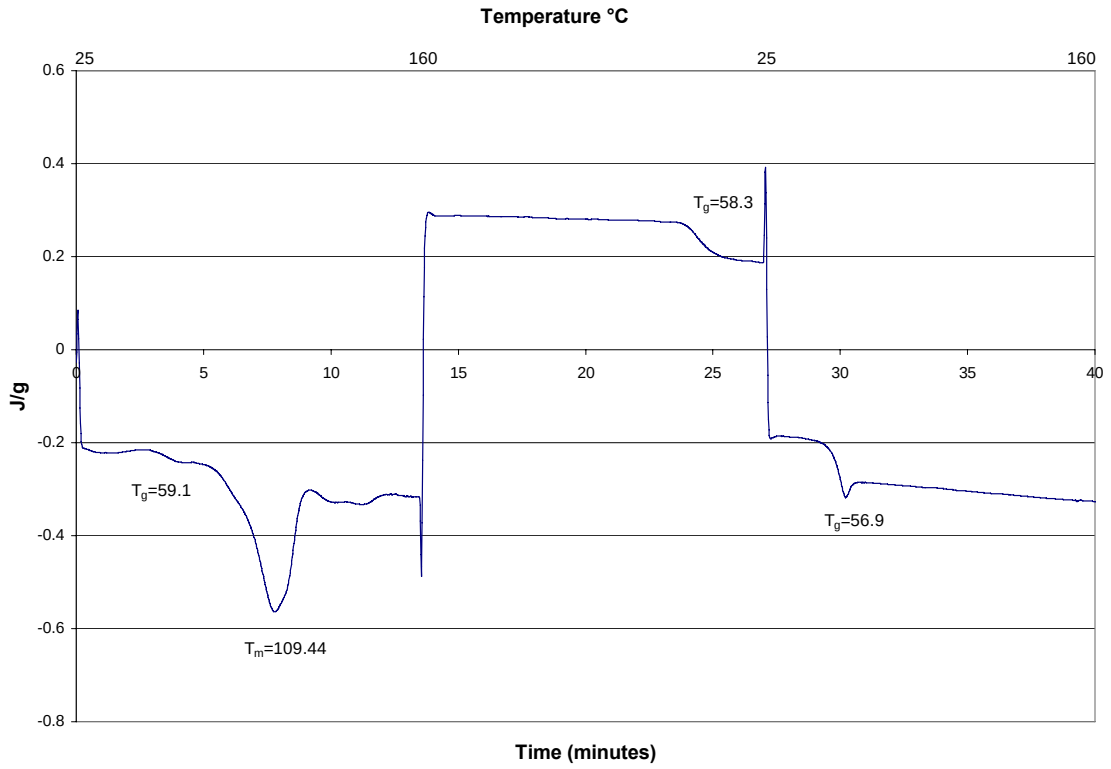

Figure 11. DSC Reheated As received 4-Phe-4 Scan

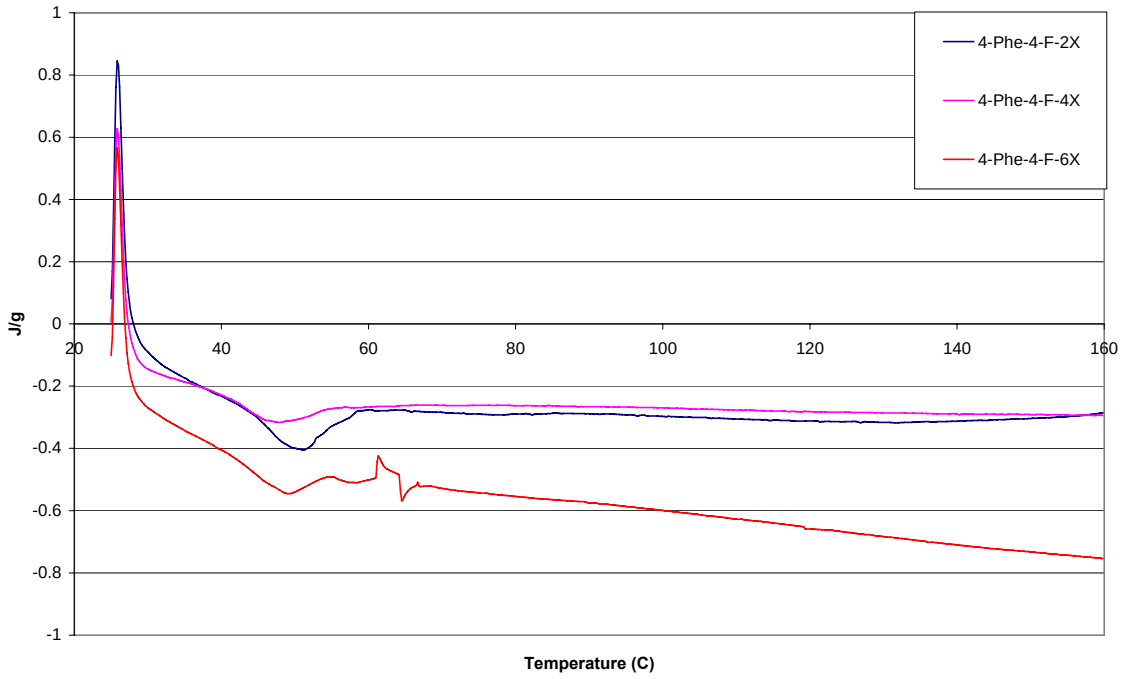

Figure 12. DSC 4-Phe-4 Drawing Comparison

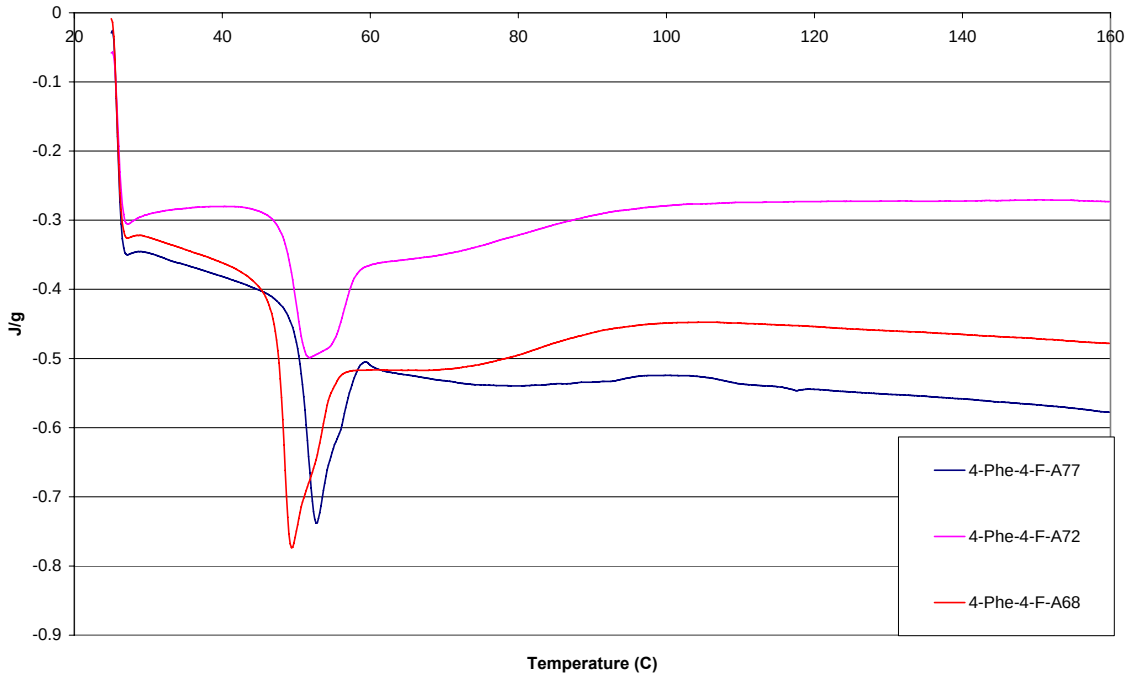

Figure 13. DSC 4-Phe-4 Annealing Comparison

The solvent effects mentioned earlier in regards to the T_m in the as received polymer scan may be the reason the T_g was higher in the as received sample than in the drawn samples. The as received 4-Phe-4 seems to have maintained a regular conformation even after the solvent has been extracted through drying. However, once it has been melted or processed, the solvent is not there to help it recrystallize. This is likely the reason for the lower T_g values in the spun fiber, and could be tested by precipitating polymer out of solution and conducting WAXD and DSC testing to determine the presence of crystallinity.

The peaks (heat absorbed) located in the T_g region of the annealed fibers require more energy than those of the drawn fibers. These peaks likely represent an enthalpic relaxation instead of the rise associated with a change in C_p normally seen. Evidently this is related to some structuring of the polymer, but not equivalent to actual crystallization, as no obvious melting point and heat of fusion is observed. There is a very broad hump in the curves for the annealed samples at temperatures well above the glass transition which likely represents relaxation of the chains.

The nucleated 4-Phe-4 samples behaved similarly to the original 4-Phe-4 spun fiber in the DSC, as is shown in **Figure 14**. The average T_g for the nucleated fibers is 47.7±0.3°C, which is slightly lower than the 52°C value of the original 4-Phe-4 fibers. Again, there is no melting peak, and nothing to indicate the presence of crystallinity in the x-ray data. The nucleating agent or the change in processing conditions appears to have slightly strengthened the polymer, but was unable to induce crystallinity.

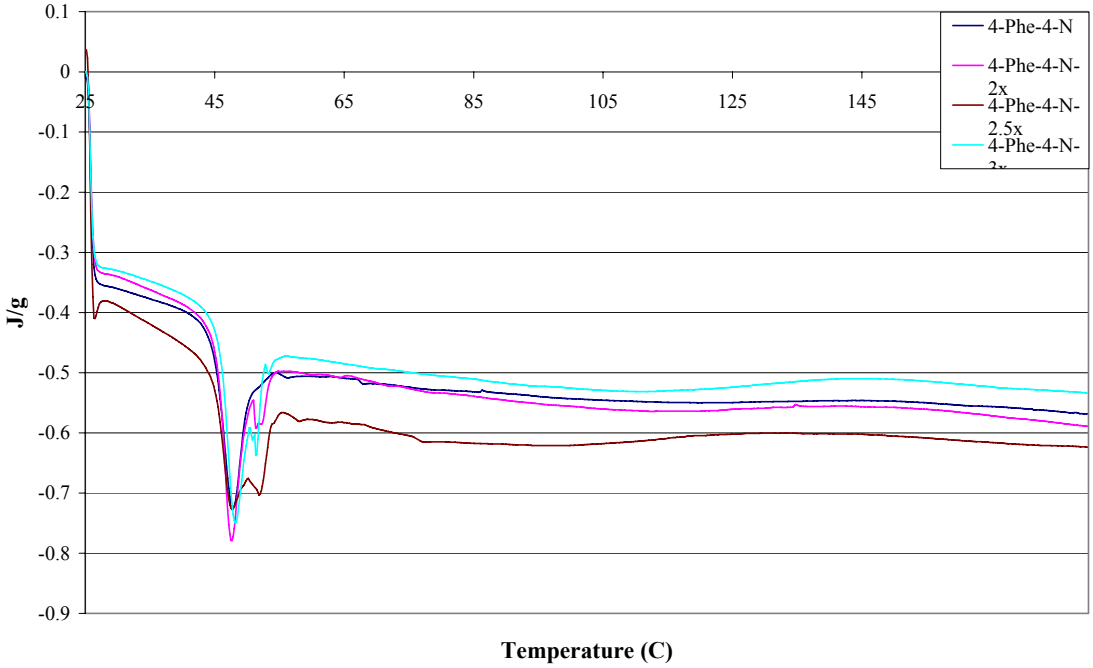

Figure 14. Nucleated 4-Phe-4 DSC Scans

4.1.8 Wide Angle X-Ray Diffraction

Images scanned from the 4-Phe-4 pinhole patterns are shown in **Figures 15** and **16**. The actual pinhole patterns are in **Figure 17**. There are two peaks of interest in some of these plots. One is a small peak corresponding to a small inner circle near the center of the image; the larger peak corresponds to the next halo out. Neither peak is sharp enough to represent appreciable crystallinity within the polymer, except in the case of the as-received polymer, which also showed a clear melting point in the DSC curve. These peaks appear in the same general area in all of the scans. The small peak occurs at approximately 11.3° 2θ, and the larger peak occurs at approximately 19.6° 2θ. The peak occurring at 11.3° 2θ in the As Received scan in **Figure 15** is more pronounced than in the other scans, and the peak at 19.6° 2θ is much more narrow than in the other samples. These are strong indicators of a higher degree of order in the as received polymer than can be attained through melt processing and drawing.

The pinhole patterns indicate that there is never really any crystallinity in the polymer after it has been melt processed. There is orientation developed in the samples, and this can be seen in the pinhole patterns in **Figure 17**. **Figure 17g** starts to look like it has some orientation, because of the 2 brighter arcs on each side of the halo. To some extent, this is also true of **Figure 17f**, but the lower draw ratio did not produce quite as dramatic an effect. This is more easily seen in **Figure 17m** which shows the azimuthal variation of intensity of the 19.6° 2θ peak for the 4x and 6x drawn samples. For an unoriented (random) sample, this intensity would be constant around the ring.

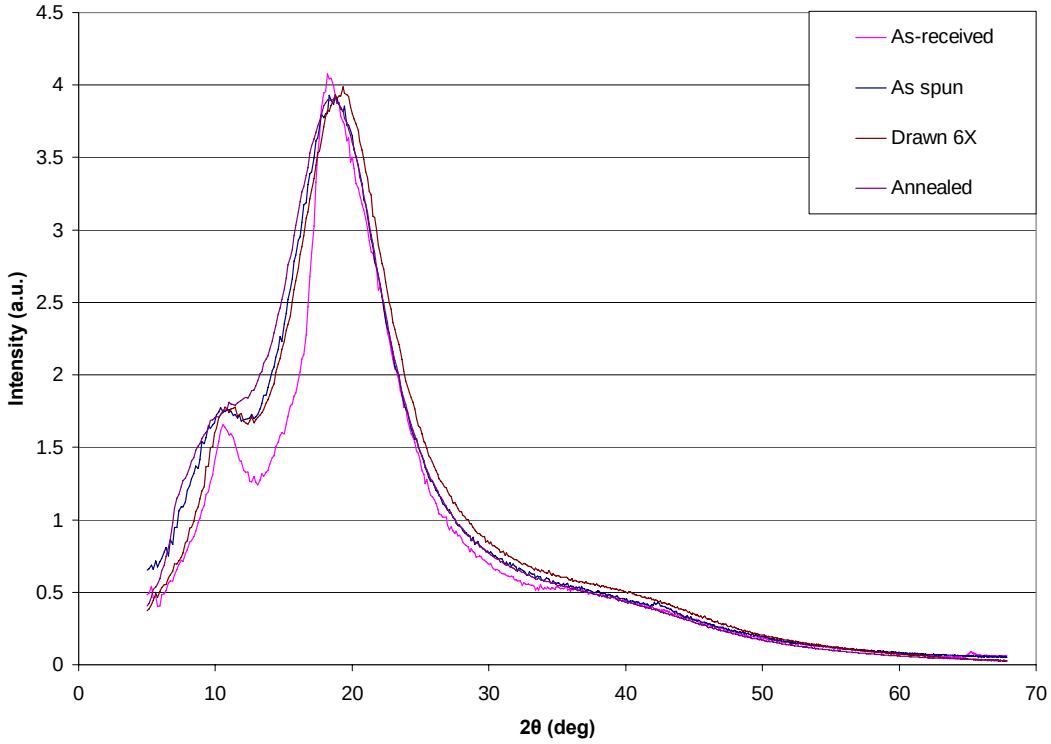

Figure 15. 4-Phe-4 WAXS Patterns

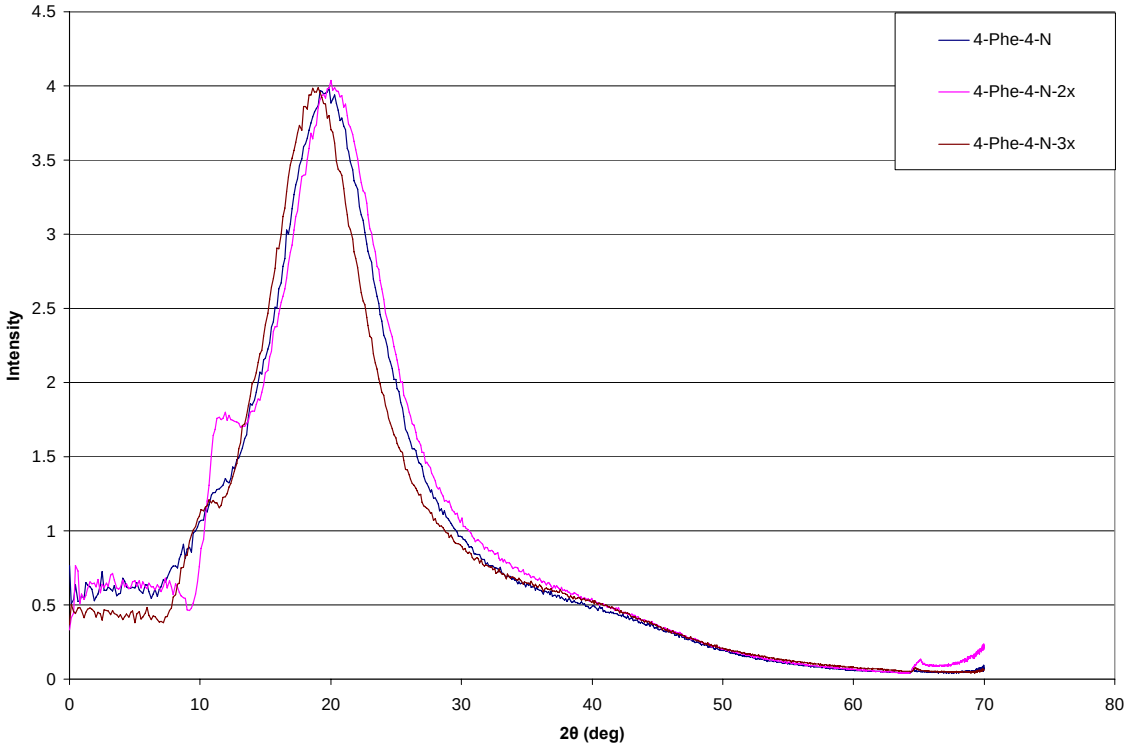

Figure 16. Nucleated 4-Phe-4 WAXD Patterns

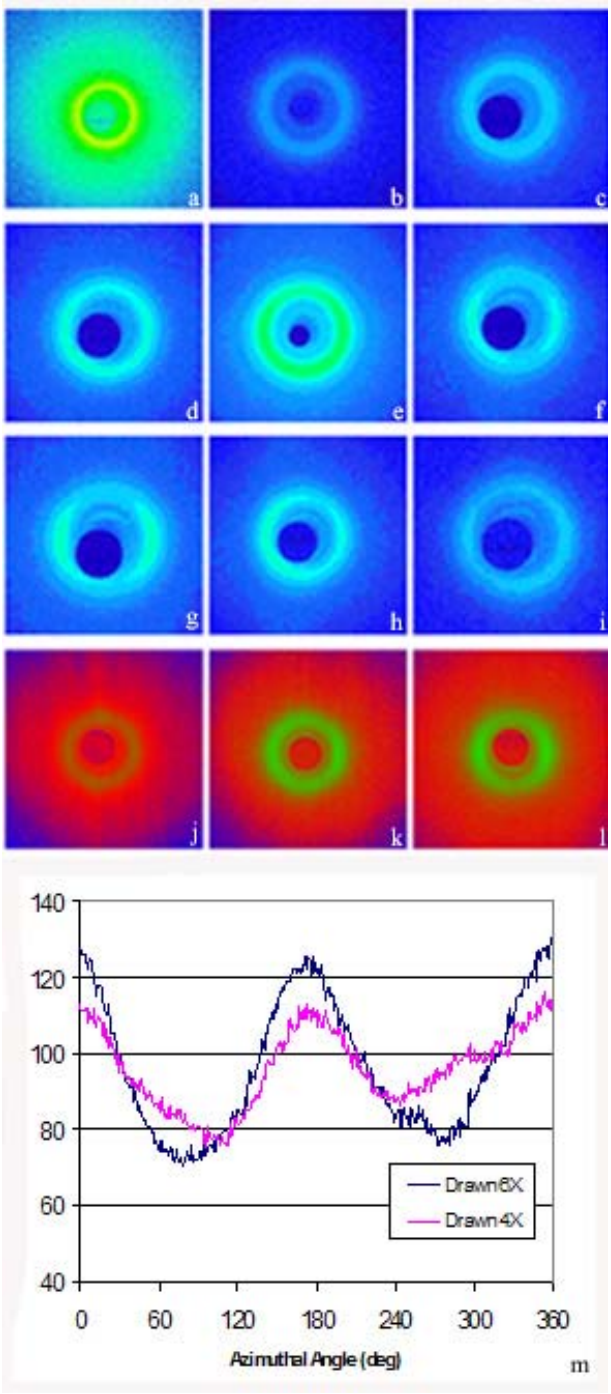

Figure 17. 4-Phe-4 Pinhole Patterns
a) As received, b) Spun Fiber, c) 77°C Annealed Fiber, d) 72°C Annealed Fiber, e) 68°C Annealed Fiber, f) Drawn 4x, g) Drawn 6x, h) Annealed 4x, i) Annealed 6x, j) Nucleated Spun Fiber, k) Nucleated Drawn 2x, l) Nucleated Drawn 3x, m) Azimuthal Scans around the 6x and 4x Pinhole Patterns

The nucleated sample that was drawn 3x in **Figure 17l** shows fairly extensive molecular orientation as a result of the processing conditions. All of the samples look amorphous, however, regardless of any modifications designed to induce crystallinity.

4.1.9 Optical and Mechanical Properties

Draw ratios were back calculated from the diameter of the drawn fiber and their birefringence values were measured. In **Figure 18**, Birefringence is plotted versus Draw Ratio for the 4-Phe-4. There is an overall trend towards the higher the draw ratio, the higher the birefringence. The charts in **Figure 19** show examples of the stress strain curves of the 4-Phe-4 as spun fiber and the 4-Phe-4 4x drawn fiber. The as-spun fiber is very brittle; exhibiting very little ductility. Drawing improved the ductility and the overall strength of the fiber substantially. The charts in **Figures 20 - 22** show trends in mechanical properties versus birefringence for the all of the tested fibers.

With the 4-Phe-4, for both the ultimate tensile strength and the yield strength, as the birefringence increases, so does that mechanical property. This trend is somewhat evident in the elastic modulus, however it is not as profound as it is in the other two cases. The use of the nucleating agent seemed to increase the fiber stiffness and decrease its ductility. The high modulus values shown in **Figure 20** relate to the stiffness, which is greatly increased from the original 4-Phe-4. Yield strength values in **Figure 21** are unchanged within reasonable error between the original and nucleated fibers. Tensile strength values are shown in **Figure 22** and are the evidence of lower elongation to break. The addition of the nucleating agent seems to have caused a stress concentration within the fibers. This leads to crack initiation under load, and results in the lower elongation to break.

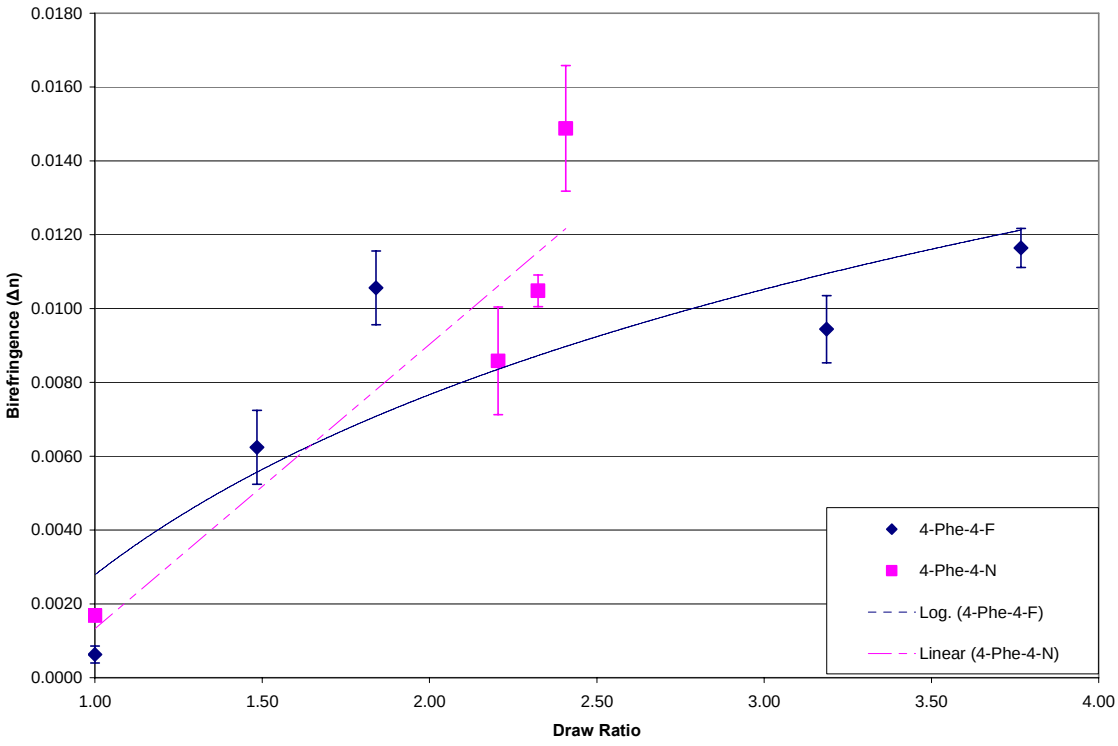

Figure 18. 4-Phe-4 Draw Ratio vs. Birefringence

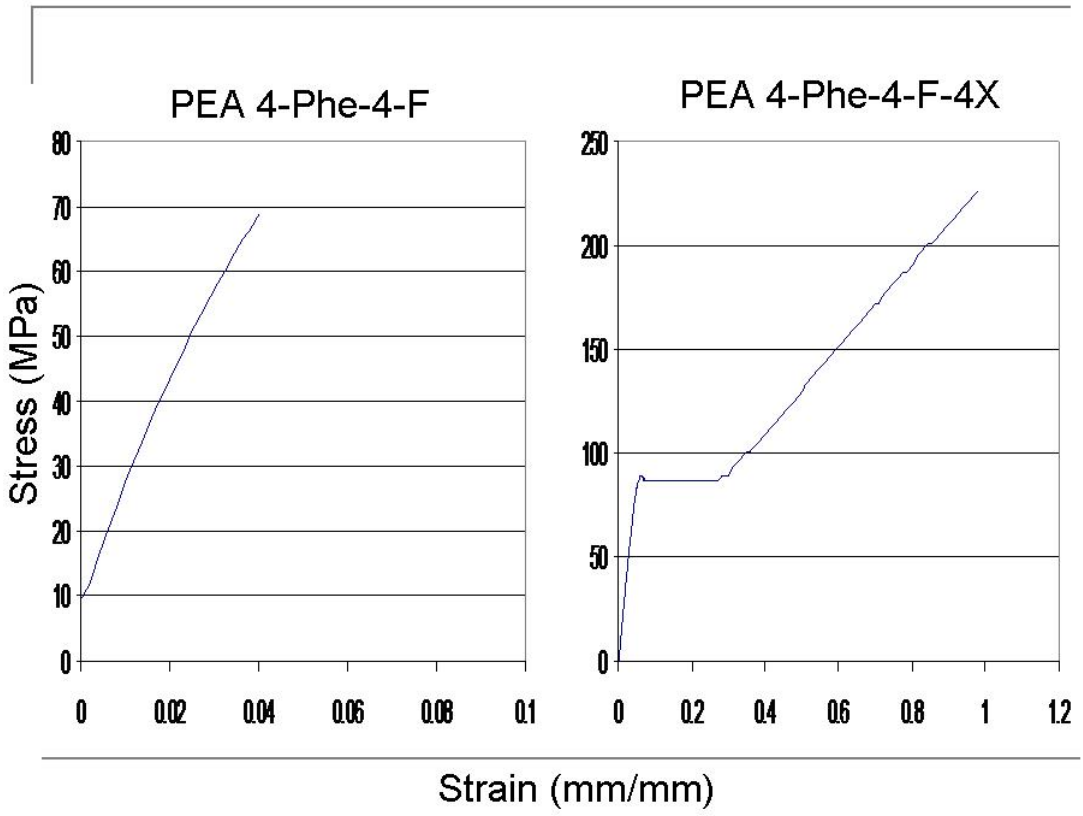

Figure 19. 4-Phe-4 Stress Strain Curves

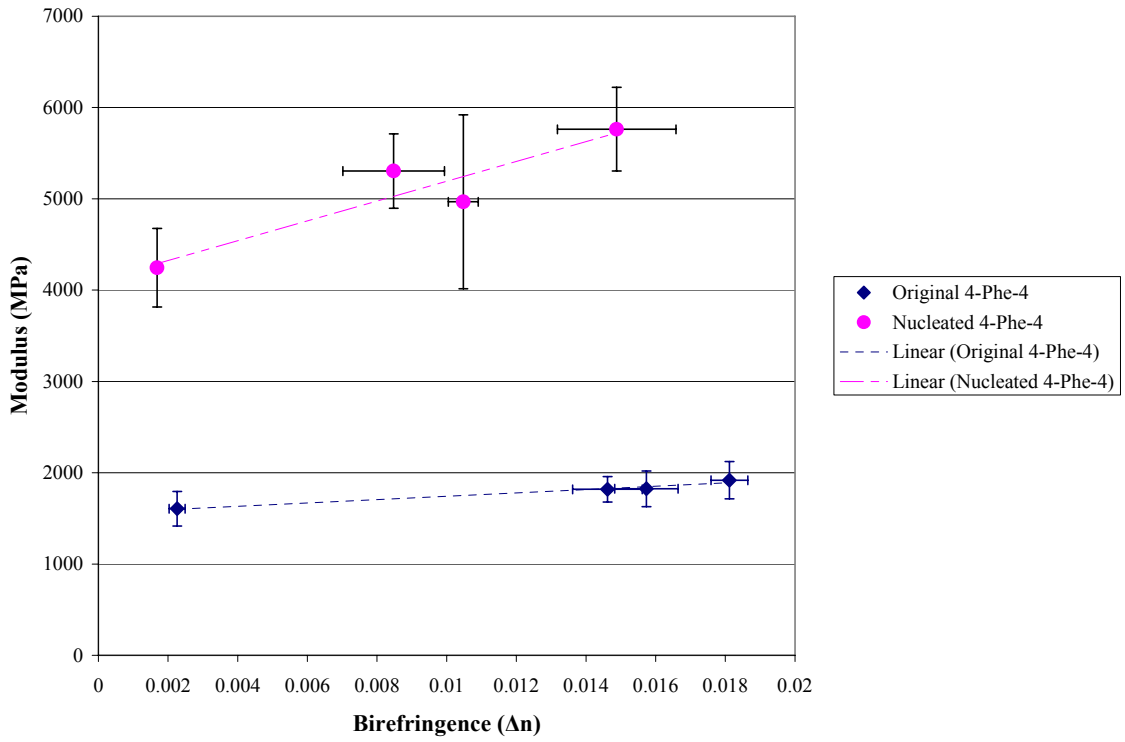

Figure 20. Modulus vs. Birefringence

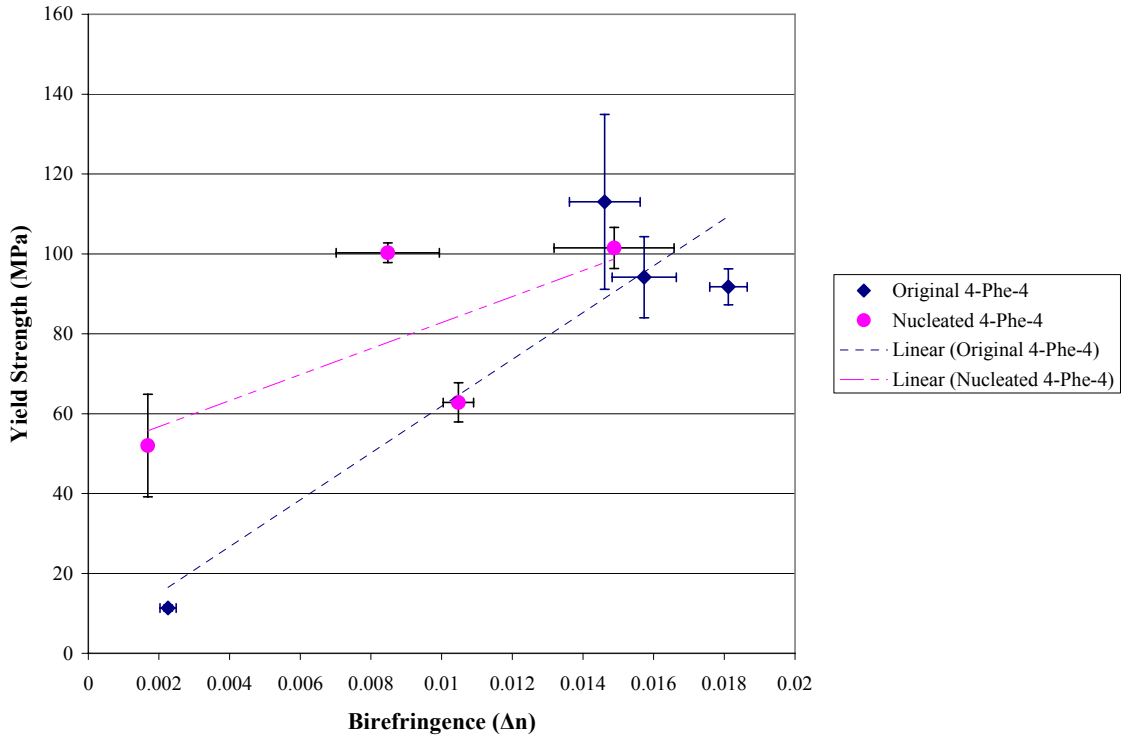

Figure 21. Yield Strength vs. Birefringence

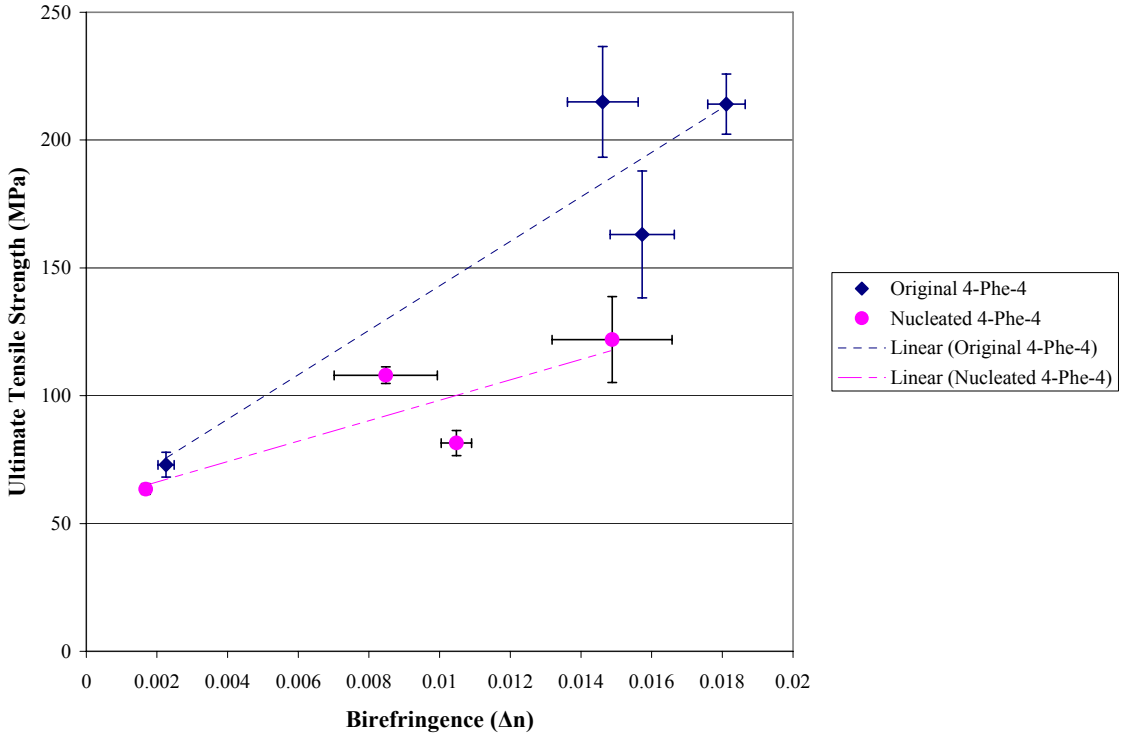

Figure 22. Ultimate Tensile Strength vs. Birefringence

4.1.10 Preliminary Shrinkage and Hydrolysis Testing

The water shrink test was conducted as another way to test the orientation of the drawn fibers and determine if crystallinity occurred during drawing. This test was conducted at 75°C. With the shrink test, the as spun fiber and annealed fibers were the least reactive, while the drawn fiber shrank a great deal. The fact that 75°C is well above the T_g and the lack of crystallinity, explains why the drawn fibers shrink to the extent that they do. Based on this, the 6x fiber could be expected to shrink up to 83%. Annealing was conducted at 68°C prior to testing. This heating suggests that while the length remained unchanged during annealing due to the sample holder, orientation was lost due to chain mobility at the higher temperatures. Since the bulk of the orientation had already been relaxed, the annealed samples were not as susceptible to shrinkage. Had there been some crystallinity, the chains oriented by drawing would have been more stable and restricted by their conformation. These results are shown in **Table 5**.

The hydrolysis test was conducted to see if degradation and orientation change could be induced by the presence of water at 37°C. Birefringence measurements were taken once the samples were removed from the water and allowed to dry. These values are given in **Table 6**. It is clear from the results that no changes in orientation took place from the exposure to water at this temperature.

4.1.11 Compression Molding

Milled 4-Phe-4 was used to create compression molded sheets of thin film. This polymer responded fairly well to the heat and pressure. The film was brittle, but not to the point that it could not be handled.

Table 5. Shrink Test Results

4-Phe-4-F		**4-Phe-4-F-6x**	
Li (in.)	6	Li (in.)	6
Lf (in.)	4.54	Lf (in.)	1.3
% change	24	% change	78
4-Phe-4-F-A		**4-Phe-4-F-A6x**	
Li (in.)	2	Li (in.)	2
Lf (in.)	1.57	Lf (in.)	0.896
% change	21	% change	55

Table 6. Hydrolysis Test Results

Birefringence (Δn)		**Diameter (μm)**
Untreated	0.0200	81.25
1 Hour	0.0215	74.75
1 Day	0.0215	81.25
5 Days	0.0219	81.25
10 Days	0.0215	78.00

While some bubbles were present in the film, much of the sheet that was used in the biaxial stretcher was free of defects. Film was successfully stretched uniaxially in constrained and unconstrained conditions. Biaxial stretching was not attempted due to problems with the machine grips and low amounts of polymer. Birefringence measurements were taken of the film, and the film was exposed to creep testing via the DMA.

4.1.12 Optical Properties of Film

The birefringence values were calculated from the retardance measurements of each sample. Draw ratio values were obtained by drawing 1 cm lines on the film samples prior to stretching. Separation of these lines was then measured to get a more accurate assessment of how the film drew. While specific draw ratios were set during machine preparations, the films did not stretch uniformly. In an effort to be more accurate, the measured draw ratios were used instead of the supposed values from the machine setup. Samples were cut from what seemed to be the most uniform parts of the film. With both the unconstrained samples and constrained samples, the expected increase in birefringence with increasing orientation is seen. These values are shown in **Figure 23**.

The values of birefringence measured for the film are lower than those found for the fiber. There are two possible reasons for this. The fibers were initially partially oriented during spinning as they were pulled at high speeds from the extruder to the take-up roll. Thus, the fibers were exposed to a two-step drawing operation. The compression molded sheets developed no orientation during compression molding, so it would make sense that they would orient less than the fiber.

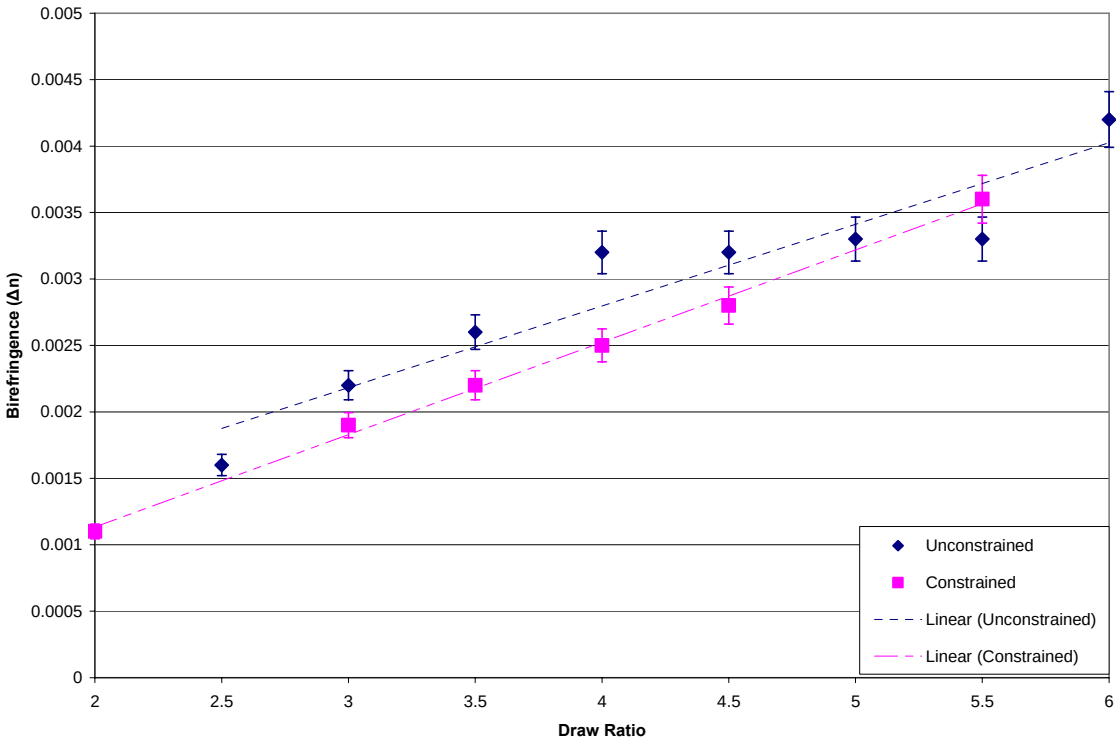

Figure 23. Draw Ratio vs. Birefringence 4-Phe-4 Film

But of greater importance, the temperature used for the fiber drawing was significantly lower than the temperature used for the film. It is likely that the increased chain mobility caused by the higher temperature resulted in a loss of overall chain orientation even though the film and fiber had similar draw ratios.

4.1.13 Dynamic Mechanical Analysis

Due to time constraints, sufficient data could not be collected at varying temperatures in order to perform time-temperature superposition. The initial load was chosen based on the yield stress results of the drawn fibers obtained during tensile testing. According to Pego, it is typical to make the applied stress 5-30% of the yield stress for biomedical polymers, however these values appeared to be too small and the sample experienced non uniform strain. [18] The load of 50% YS provided realistic results, even though 50% is much higher than the anticipated load. Tests were conducted at 37°C to simulate body conditions. The chart shown in **Figure 24** indicates that both the constrained and unconstrained film samples undergo secondary creep during static loading. The values for creep compliance are shown in the chart in **Figure 25**. The constrained film samples appear to creep at a faster rate than their unconstrained counterparts. This is likely due to the slight orientation in the transverse direction from contact with the grips in the stretcher, and slightly lower orientation in the primary stretch direction. The unconstrained film is all oriented in the direction of stress, and is therefore slightly more resistant to creep than the constrained film.

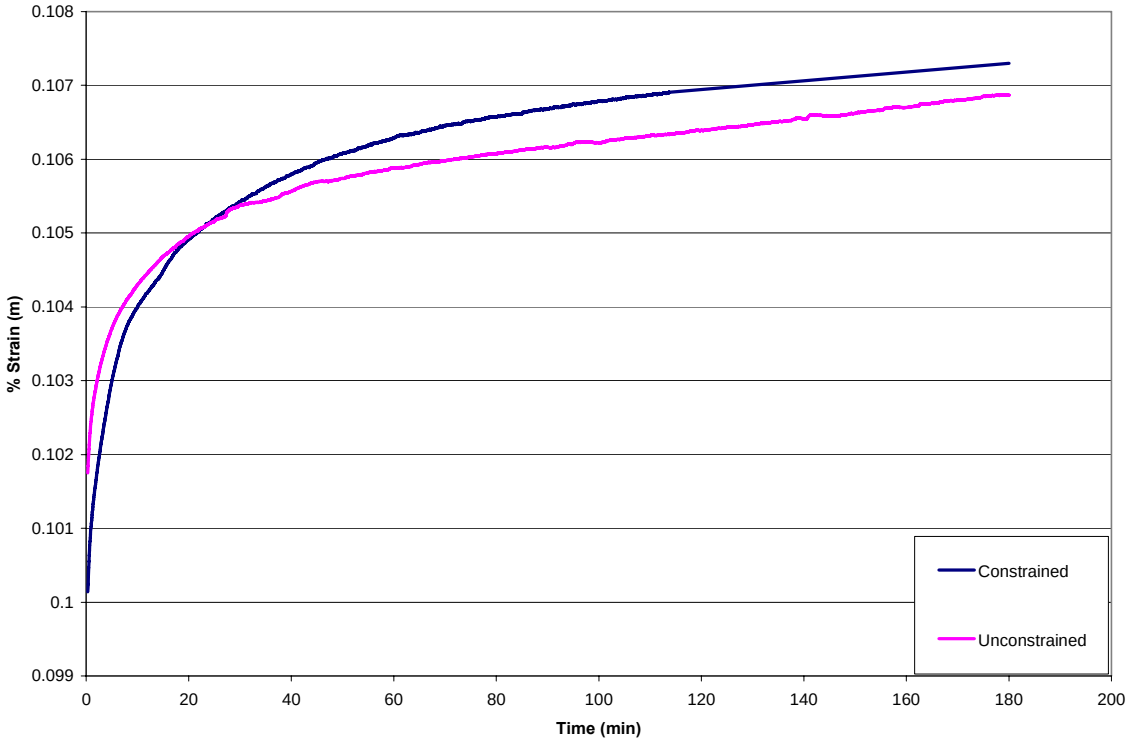

Figure 24. %Creep Strain vs. Time

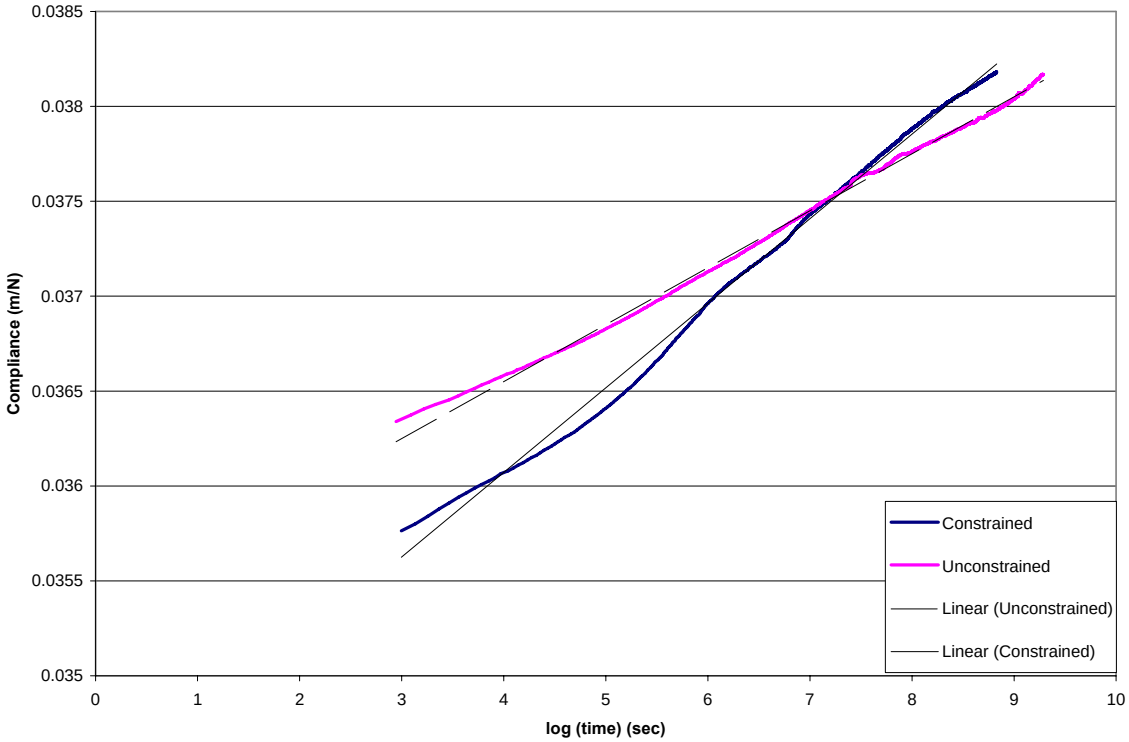

Figure 25. Creep Compliance vs. Log Time

4.2 PEAs 4-Phe-Das and 8-Phe-Das

4.2.1 Melt Flow Indexing

Melt flow experiments were conducted on the 4- and 8-Phe-Das polymers, however, both moved through the barrel too quickly to gain an accurate melt flow rate measurement. Temperature trials were run from 110-150°C. Based on the quality of the extrudate, a die temperature of 135°C was chosen for melt spinning.

4.2.2 Dilute Solution Viscosity

The intrinsic viscosity of the 4- and 8-Phe-Das polymers was quite low, and likely the reason for the poor processability and brittleness. The viscosity value sent by Dr. Chu was 0.2 dl/g. This is very close to the measured values of 0.27 dl/g for all das samples tested.

4.2.3 Melt Spinning

The 4-Phe-Das and 8-Phe-Das as received polymers were dried extensively prior to melt spinning to remove solvent and excess water. They were dried at 50°C, which was chosen based on DSC results. Prior to drying, the as received polymers lay in flat, hard sheets that after being broken into smaller pieces would have theoretically been easy to load into an extruder. As the solvent and water gases were released in the vacuum oven, however, the polymer expanded and became very soft and airy (i.e. full of bubbles). These pieces would be difficult to steadily pass through the extruder in the hopes of making decent fiber samples. Instead, a larger die was initially used and the polymer was extruded into rod and pelletized. The pellets were much more manageable

when filling the barrel of the extruder, and were not in danger of jamming the screw at the entrance of the hopper.

Once the pellets were formed, two bobbins were wound for each polymer. The diameters were significantly larger than the 4-Phe-4 fiber due to the slower spinning conditions needed to keep the spin-line from breaking. The diameter for the as spun fiber ranged primarily from 220-270 μm. A small amount of 4-Phe-Das was wound at higher speeds, and produced fibers of diameter 75 μm.

4.2.4 Drawing and Annealing

After spinning the 4- and 8-Phe-Das, drawing was attempted in the hopes of improving the mechanical properties of the fibers and reducing their brittleness. However, since the fibers were so brittle, it was extremely difficult to wind them through the drawing machine. The fiber repeatedly broke as it was coming off of the bobbin and as it was being wound onto the warm rollers on the machine. To avoid problems with the bobbin, small segments were then tested. These segments were 2 feet in length with a 2 inch section marked in red. These segments were wrapped repeatedly around the warm rolls with an attempt at keeping tension on both ends of the fiber. In this case, the fiber appeared to draw, however further examination of the 2 inch area shows that this was not the case. Instead of drawing, the fibers looked like they were necking in places and beginning to fail. The diameter throughout the 2 inch section was inconsistent. It is unknown at this point if the fiber can be drawn at all. It is possible that passing the fiber through a warm tube before attempting to wrap it around the rolls might reduce breakage at that end, but that does not solve the problem of the fiber breaking as it is pulled from the bobbin.

4- and 8-Phe-Das Fibers were annealed, successfully, at both 65° and 70° C. Time trials were conducted at both of these temperatures to see how the fibers reacted. These times were 60 minutes, 90 minutes, and 4 hours. Upon completion of these trials, it seems that the time did not matter as much as the temperature when attempting to reduce orientation. The 4-Phe-Das seemed to respond to both temperatures, contracting as much as possible in the rack they were mounted in. The 8-Phe-Das fibers did not show much change, and it is possible that a higher temperature is needed for these fibers. These annealed samples were tested by DSC and WAXD, and tensile testing and birefringence measurements were made.

4.2.5 Differential Scanning Calorimetry

A DSC scan for the as-received 4-Phe-Das polymer is shown in **Figure 26**. The Tg for this sample is about 40.0°C. There is an endothermic peak at approximately 104°C. On first examination, it appeared that the endotherm represented melting of crystals. But since the X-ray pattern of this sample indicates there is no crystallinity, another explanation is needed. The value of Tg for this as received 4-Das polymer is substantially lower than for the as-spun and annealed samples. This behavior is most likely caused by the solvent and water retained in the as received Das sample. When heated in the DSC, the retained solvent and water initially plasticized the polymer. The release of the solvent and water vapor evidently account for the endotherm. A somewhat similar behavior is found for the 8-Das sample, and is interpreted the same way.

The average Tg for both the as received 4- and 8-Phe-Das is 40°C, and the average for the spun fibers for both is 57.9±0.5°C.

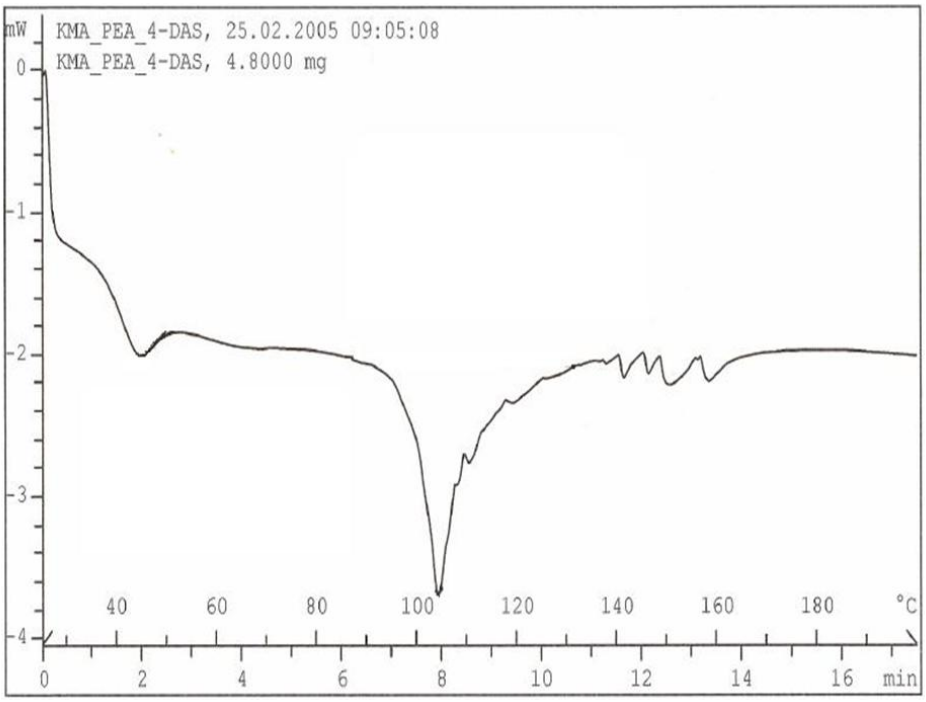

Figure 26. 4-Phe-Das As received DSC Scan

Figure 27 shows DSC scans for the different annealing treatments for the 4-Phe-Das polymer, and **Figure 28** shows the same comparison for the 8-Phe-Das. The scans do not show much difference between samples. Both the as-spun and annealed scans exhibit a hump beginning around 105°C and ending around 160°C. These humps in the curve appear to indicate instability within the chains as they relax during heating. This is also evident by the lack of a solid baseline in the annealed comparison. This could be due to retained solvent, causing an endotherm as they are released while the polymer softens. It may also be due to severe contraction of the pieces of fiber resulting in loss of contact with the pan during testing.

4.2.6 Wide Angle X-Ray Diffraction

All of the 4- and 8-Phe-Das wide angle x-ray diffraction patterns are similar with no exceptions. This statement includes the as received polymer, the as-spun fiber, and the annealed fibers. The 2θ scans for the as received and spun 4-Phe-Das are shown in **Figure 29**, and the scans for the as received and spun 8-Phe-Das are shown in **Figure 30**. The pinhole patterns are included in **Figure 31**. There is no crystallinity present within any of the fiber samples tested, nor do they appear to have any chain orientation. It is possible that were drawing an option, there would be some orientation within the fibers, but the fibers were so brittle, that drawing was not possible.

4.2.7 Optical and Mechanical Properties

The birefringence values are included in Table 7. These values are quite low, indicating virtually no orientation within the fibers. This agrees with the x-ray patterns in **Figure 31**.

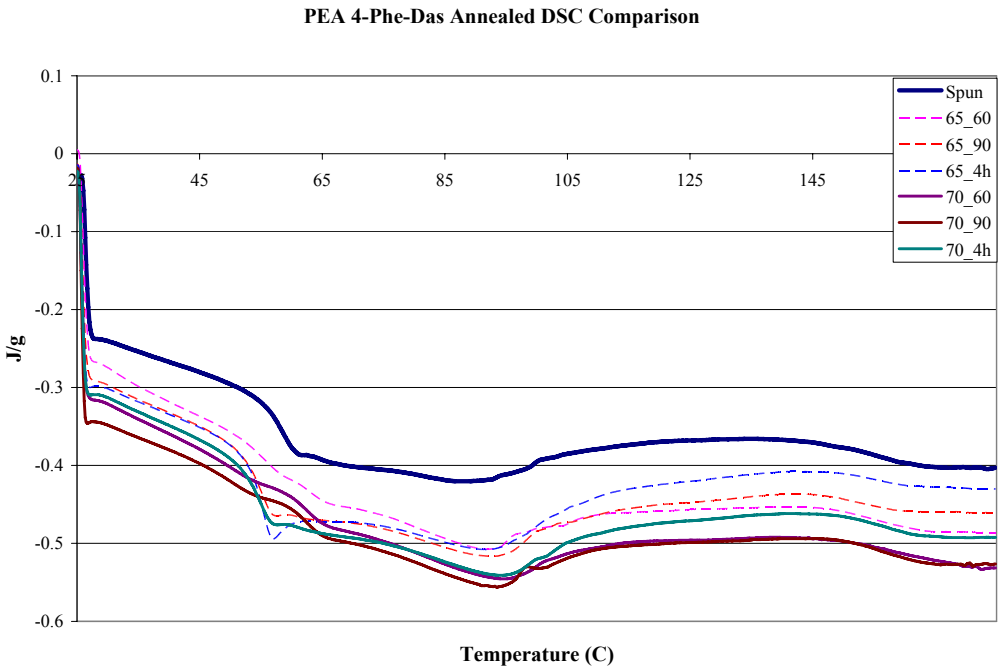

Figure 27. 4-Phe-Das DSC Annealing Comparison

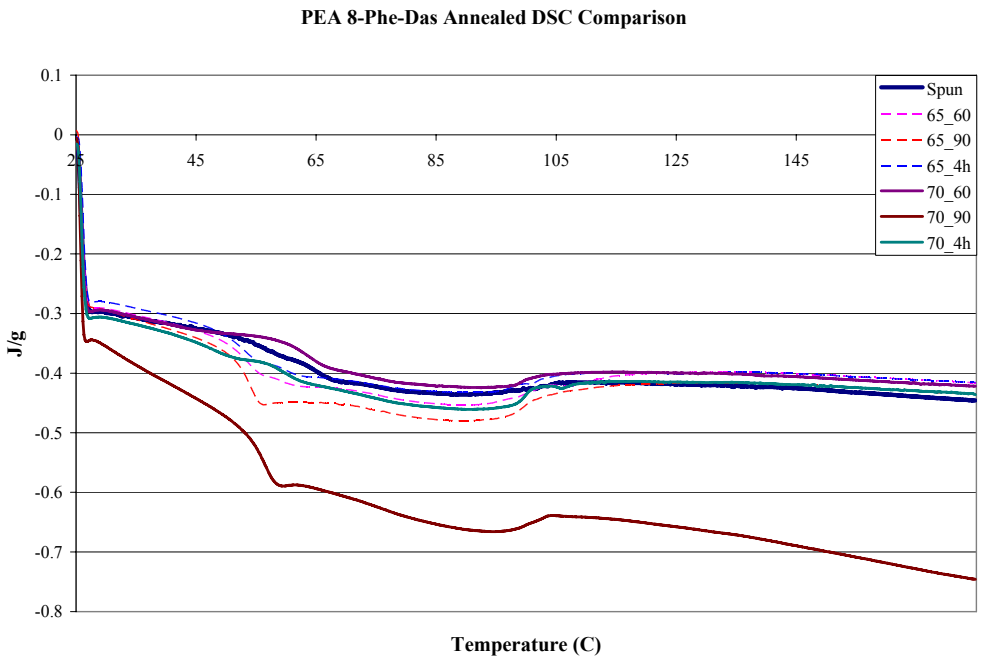

Figure 28. 8-Phe-Das DSC Annealing Comparison

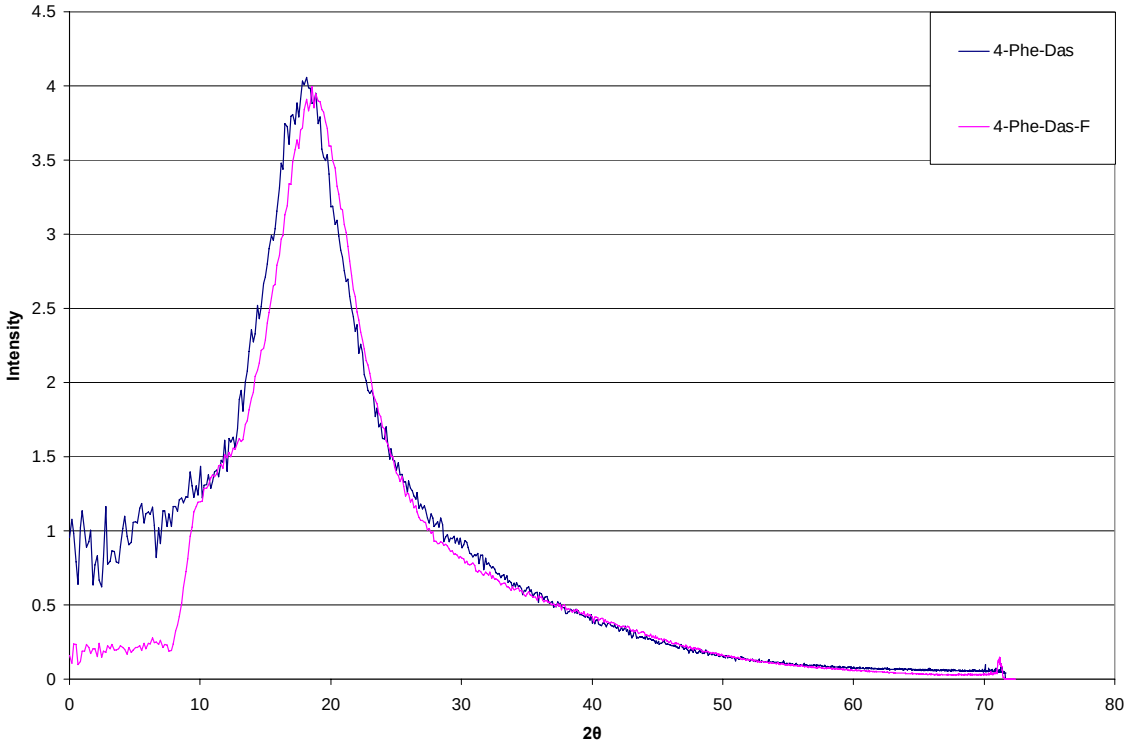

Figure 29. 4-Phe-Das WAXD Patterns

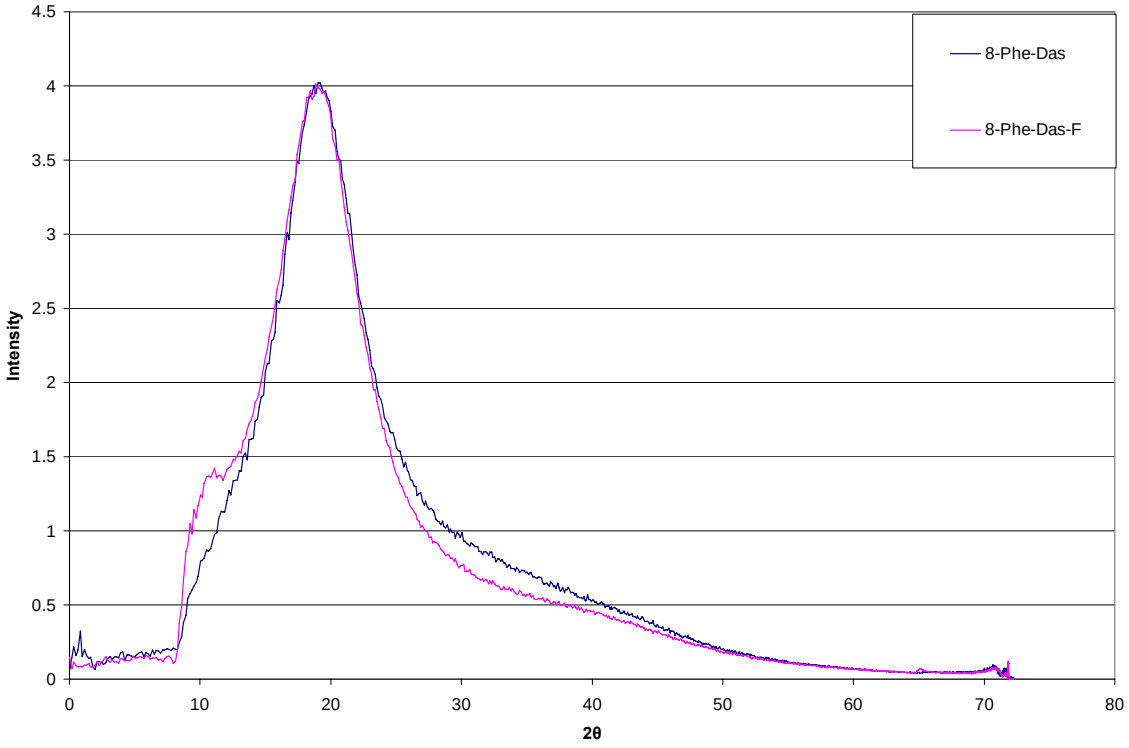

Figure 30. 8-Phe-Das WAXD Patterns

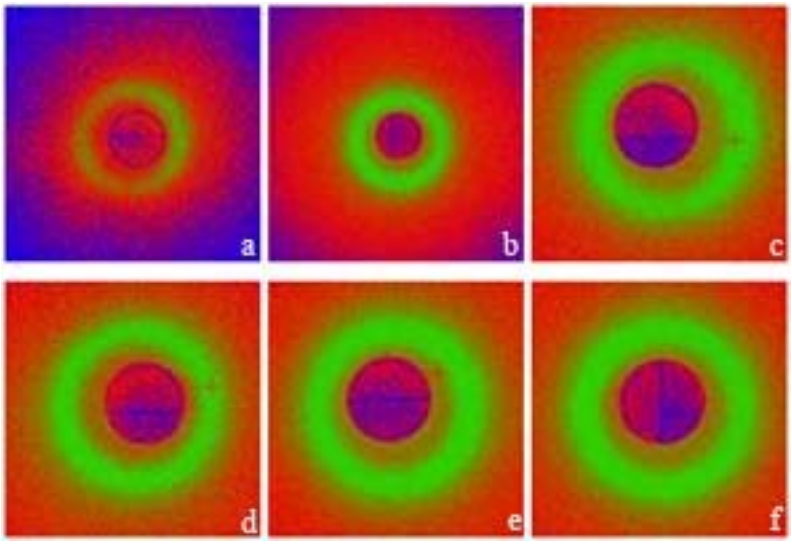

Figure 31. 4- and 8-Phe-Das WAXD Pinhole Patterns
a) 4-Phe-Das As received, b) 4-Phe-Das Spun Fiber, c) 4-Phe-Das Annealed Fiber, d) 8-Phe-Das As received, e) 8-Phe-Das Spun Fiber, f) 8-Phe-Das Annealed Fiber

Table 7. 4- and 8-Phe-Das Optical and Mechanical Data

Sample	Birefringence (Δn)	Modulus (MPa)	Tensile Strength (MPa)
4-Phe-Das-F	0.00341±0.0028	2337±518	100.02±7.7
4-Phe-Das-F-A65	0.0014±0.0001	1306±206	58.38±9.7
4-Phe-Das-F-A70	0.00124±0.0001	1214±55	44.57±12.1
8-Phe-Das-F	0.00103±0.0003	1761±407	63.21±6.2
8-Phe-Das-F-A65	0.00105±0.0001	1315±265	56.12±11.5
8-Phe-Das-F-A70	0.00117±0.0001	1517±325	66.5±13.9

The optical and mechanical properties of the 4- and 8-Phe-Das did not appear to remarkably change following the annealing process. The birefringence values for the as spun and annealed fibers are quite low, indicating very little chain orientation. The values for modulus and ultimate tensile strength listed in **Table 7** are very close in value to the as spun 4-Phe-4. Yield stress could not be calculated, because the fibers did not yield. They broke almost immediately upon loading. The modulus, tensile, and birefringence values listed are averages of six samples.

Chapter 5. Summary and Conclusions

Following melt flow indexing trials, the three poly(ester amide)s were processed into fiber by melt spinning. The extrusion parameters were decided upon by both melt flow indexing and DSC. Die temperatures of 181°, 187°, and 185°C were used for the pure 4-Phe-4 and 150°C was used for the nucleated polymer. 4-Phe-Das and 8-Phe Das were processed at die temperatures of 135 and 140°C respectively. Post extrusion drawing and annealing were conducted on the 4-Phe-4 fibers in an attempt to induce orientation and crystallinity. Fibers were drawn at temperatures of 56°C and 48°C, and subjected to annealing temperatures of 77°, 71°, and 68°C under constant length. The nucleated fibers were drawn at 28°, 44°, and 46°C, but were not annealed. The 4-Phe-Das and 8-Phe-Das fibers were annealed at 65° and 70°C, but were unable to be drawn due to their extreme brittleness.

Drawing leads to an increase in the mechanical and optical properties in both the original and nucleated 4-Phe-4. This is due to orientation of the polymer chains in the load direction. WAXD pinhole patterns provide a visual representation of the amorphous polymer becoming oriented following drawing. The addition of the sodium benzoate increased the modulus of the fibers, however it decreased the tensile strength. This implies that the nucleating agent increased the fiber stiffness, but provided stress concentrations within the fiber that lead to a lower elongation to break.

Spun fibers of 4-Phe-4 exhibit a decrease in T_g from the as received polymer value. This is likely a result of the solvent used during synthesis. The as received 4-Phe-4 seems to have formed a regular conformation due to solvent effects during synthesis,

and has kept this conformation through drying and release of any remaining solvent. Once melted, however, there is nothing to push the polymer back into an ordered structure. This would explain both the decrease in T_g, as well as the loss of T_m. The 4-Phe-Das and 8-Phe-Das did not exhibit this solvent induced regular conformation. Once the solvent had been released, the as received and spun fibers maintained similar thermal profiles. The expected increase in T_g occurred following processing.

4-Phe-4 films were successfully compression molded at 140°C, and were drawn at 110°C. Due to higher drawing temperatures and no induced orientation during molding, these films have lower birefringence values than the drawn fiber. These film samples also underwent secondary creep at 37°C. Given more time, data could be collected for longer time periods and at different levels of stress to determine at what point, the material would fail under creep conditions.

The synthesis carried out by Dr. Chu likely resulted in the formation of an atactic polymer, which would explain why crystallization could not be induced. To improve the properties of the 4-Phe-4, stereoregularity should be induced during synthesis. Another recommendation during synthesis would be to increase the molecular weight. Producing polymer of higher molecular weight would increase the spinnability and result in a less brittle fiber.

Chapter 6. Future Work

To achieve a better understanding of the effects of solvent, DSC and WAXD tests should be conducted on polymer that has been precipitated from solvent. Depending on these results, solution spinning could be revisited with a better understanding of the parameters needed to produce fiber. Solution spinning still appears to be the most plausible method of producing semi-crystalline fibers with the current 4-Phe-4 polymer.

With more polymer, the melt spinning parameters could be revised and improved upon. The parameters used during spinning with the nucleating agent were a vast improvement over the original conditions. These parameters likely provided the greatest impact upon the changes in modulus and the easier drawing. Another round of testing could improve these properties further, and without the stress concentrations caused by the nucleating agent, testing could be done to determine if elongation to break and ultimate tensile strength increase as a result of better spinning conditions.

Finally, a more comprehensive creep study would be useful in determining appropriate medical applications for the 4-Phe-4. The film samples should be tested under various loads that are applicable to real world situations. Time and temperature trials would be useful as well to gain overall knowledge of how the polymer behaves.

REFERENCES

REFERENCES

1. H. Alexander, J. B. Brunski, S. L. Cooper, L. L. Hench, R. W. Hergenrother, A. S. Hoffman, J. Kohn, R. Langer, N. A. Peppas, B. D. Ratner, S. W. Shalaby, S. A. Visser, and I. V. Yannas, "Classes of Materials Used in Medicine," in *Biomaterials Science*, B. D. Ratner, A. S. Hoffman, F. J. Shoen, and J. E. Lemons, ed. (Academic Press, California, 1996), pp. 50-72.

2. H. F. Mark, N. M. Bikales, C. G. Overberger, G. Menges, and J. I. Kroschwitz, *Encyclopedia of Polymer Science and Engineering*, Vol. 9 (Wiley, New York, 1987). pp. 486-501.

3. R. S. Benson, "Introduction to Biomaterials" Biomaterials Class Notes, the University of Tennessee, Spring 2003.

4. A. R. Coury, R. J. Levy, C. R. McMillin, Y. Pathak, B. D. Ratner, F. J. Schoen, D. F. Williams, and R. L Williams, " Degradation of Materials in the Biological Environment," in *Biomaterials Science*, B. D. Ratner, A. S. Hoffman, F. J. Shoen, and J. E. Lemons, ed. (Academic Press, California, 1996), pp. 243-258.

5. Y. He, Z. Qian, H. Zhang, X. Liu, "Alkaline degradation behavior of polyesteramide fibers: surface erosion," *Colloid Polymer Science* Vol. 282, 2004. pp 972-978.

6. R. Katsarava, V. Beridze, N. Arabuli, D. Kharadze, C. C. Chu, C. Y. Won, "Amino acid-based bioanalogous polymers. Synthesis, and study of regular poly(ester amide)s based on bis(α-amino acid) α,ω-alkene diesters, and aliphatic dicarboxylic acids," *Journal of Polymer Science: Part A – Polymer Chemistry* Vol. 37, 1999. pp 391-407.

7. C.C. Chu, G. Tsitlanadze, T. Kviria, M. Machaidze, N. Djavakhishvili, and R. Katsarava, "Biodegradation of amino-acid based poly(ester amide)s: *in vitro* weight

loss and preliminary *in vivo* studies" *Journal of Biomaterials Science – Polymer Edition* Vol. 15, 2004. pp 1-24.

8. C. C. Chu, J. E. Spruiell, "Biologically active bioabsorbable fibers for biomedical uses" *National Textile Center Research Briefs – Materials Competency* M03-CR04, 2006.
9. J.R.A. Pearson, *Mechanics of Polymer Processing*, (Elsevier, New York, 1985), pp. 424-472.
10. J.E. Spruiell, "Structure Formation During Melt Spinning," in *Structure Formation in Polymeric Fibers*, D. R. Salem ed. (Hanser, Cincinnati, 2001), pp. 6-26.
11. P.C. Powell, *Engineering with Polymers*, (Chapman and Hall, New York, 1983) pp. 253-269.
12. A. Ziabicki, *Fundamentals of Fibre Formation: The Science of Fibre Spinning and Drawing*, (Wiley, New York, 1976), pp. 250-267.
13. Peacock, Andrew. "Characterization and Testing" in *Handbook of Polyethylene: Structures, Properties, and Applications*. (Dekker, New York, NY 2000) pp. 350-351.
14. K. Kit, "Measuring birefringence of a polymer film" *MSE Special Topics Class Notes*, The University of Tennessee, Spring 2004.
15. Cambridge Polymer Group, "The Theory of Birefringence" www.campoly.com CPGAN #014, 2004.
16. C. C. Chu, J. E Spruiell, "Biologically active bioabsorbable fibers for biomedical uses" *National Textile Center Proposal* Project # M03-CR04 FY2004.
17. H. Song "Melt Spinning of Polyester Amide Polymers," Summer Research Project, (The University of Tennessee, Knoxville, 2003).

18. A. P. Pego, D. W. Grijpma, and J. Feijen, " Enhanced mechanical properties of 1,3-trimethylene carbonate polymers and networks" *Polymer* Vol. 44, 2003. pp. 6495-6504.
19. Y. Lin, J. Zhou, and J. Spruiell, "The effect of pigments on the development of structure and properties of polypropylene filaments," *ANTEC*, 1991. pp. 1950-1954.
20. M. Walker and A. Karim, "Mapping the effects of a nucleating agent on polymer crystallization," NIST: Multivariant Measurement Methods, 2002. pp. 1.

Vita

Katherine Atchley was born in Cleveland, TN on September 13, 1982. She received her bachelor's degree in Biomedical Engineering from the University of Tennessee in May of 2004. She enrolled in the Polymer Engineering program in the Materials Science and Engineering Department at the University of Tennessee in the summer of 2004, and received her Master degree in December of 2006.